Metrology of flocculated systems

Characterization of flocculation in a model suspension by a variety of devices.

Master's Thesis

Chair of Building Materials and Ceramics

presented by

Matthäus Haider

submitted in

Leoben at the 15.01.2013

Kurzfassung

Im Rahmen der Masterarbeit wurde das Flockungsverhalten einer Modellsuspension durch eine Vielzahl an unterschiedlichen Messgeräten beobachtet. Dabei wurden Veränderungen im Rheologieverhalten mit dem Flockungszustand der Suspension in Verbindung gesetzt. Das rheologische Verhalten der Modellsuspension wurde mit Hilfe von einem Rheometer, sowie der Magnetresonanztomographie gekoppelt mit einem Rheometer, analysiert.

Als Modellsuspension wurde Kalziumkarbonat Durcal 5 in unterschiedlichen Verhältnissen mit einer Mischung die zu 70 % aus Glukose und zu 30 % aus vollentsalztem Wasser besteht, verwendet. Durch den Einsatz von Kalziumkarbonat wurden mögliche Rheologieveränderungen der Suspension durch Hydratation von Zementphasen eliminiert. Die Glukose diente zur Verhinderung der Sedimentation von Feststoffanteilen.

Das Flockungsverhalten wurde anhand folgender Messgeräte im Hinblick auf deren Eignung zur Beobachtung von Flockungs- und Strukturformungsprozessen in dichten undurchsichtigen Suspensionen getestet: Durchlichtmikroskop, Konfokalmikroskop, Lasergranulometer, Fokussierte Laserrückstreuung (FBRM®), Partikelvisualisierung und -messung (PVM®), Röntgen - Mikrotomographie und multiple Lichtstreuung (Turbiscan).

Durch die Anwendung der unterschiedlichen Geräte und Messmethoden konnten wertvolle Informationen bezüglich dem Flockungsverhalten in dichten undurchsichtigen Suspensionen gewonnen werden. Mit Hilfe vom Durchlichtmikroskop wurden Flockengröße und Flockenform gemessen. Das Lasergranulometer ermöglichte die Anaylse der Entwicklung der Flockengrößen mit der Zeit. Anhand der Messungen mit dem Bruker Minispec konnte eine mögliche Flockung durch die Messung von Veränderungen in der örtlichen Partikelkonzentration festgestellt werden. Durch Rheometermessungen war es möglich, das Flockungsverhalten mit dem Rheologieverhalten zu koppeln. Zusätzlich wurden diese Ergebnisse durch Geschwindigkeitsprofil- und Konzentrationsprofilmessungen an der Magnetresonanztomographie mit einem Rheometer ergänzt.

Die Messungen mit der fokussierten Laserrückstreuung (FBRM®), der Partikelvisualisierung und -messung (PVM®) und der Röntgen - Mikrotomographie müssen weiter optimiert werden. Das Turbiscan hat sich für Beobachtungen am Flockungsverhalten als ungeeignet erwiesen.

Abstract

Within the scope of the Master's thesis, the suitability of a variety of laboratory devices was tested on their capability to characterize flocculation in a model suspension. The objective was to link the change in rheology with the change in fluid structure. The change in rheology was measured by a standard laboratory rheometer. Additional information was gained by the testing of the magnetic resonance imaging coupled with a rheometer.

As a model suspension, calcium carbonat Durcal 5 mixed in different ratios with a mixture of 70 % glucose and 30 % water, was used. By the application of calcium carbonat, the impact of change in rheology by cement hydration could be eliminated. Glucose helped to avoid sedimentation in the suspension.

Flocculation was tested with the help of the following laboratory devices: Transmitted light microscopy, Confocal microscopy, Laser particle sizer, Focused beam reflectance measurement (FBRM®), Particle vision microscopy (PVM®), X-ray microtomography and Static multiple light scattering (Turbiscan), to evaluate their suitability to follow an evolution process of flocculation in a dense opaque suspension.

Applying different devices on the model suspension enabled to gain useful information to study flocculation in a dense opaque suspension. By the help of the transmitted light microscope, floc size and floc shape could be measured. With the Laser particle sizer it was possible to study the evolution of floc size with time. At the Bruker Minispec, a flocculation process was observed with the measurement of local change in particle concentration with time. Based on the rheology measurements at a rheometer, the flocculation process could be coupled with the change of rheology properties of the suspension. Additional results were obtained by concentration and velocity profile measurements at the magnetic resonance imaging coupled with a rheometer.

The measurement at the Focused beam reflectance measurement (FBRM®), Particle vision microscopy (PVM®) and X-ray microtomography has to be further improved. Turbiscan turned out to be not capable to measure an floccs evolution process.

Acknowledgment

I gathered countless numbers of new experiences during my six month internship at Ecole des Ponts ParisTech - Laboratory Navier .

Firstly I want to thank Prof. Xavier Chateau and Julie Goyon for all their knowledge and support with words and advice during my master's thesis.

Then I would like to express my gratitude to Helene Lombois Burger and Fabrice Toussaint from Lafarge for the outstanding opportunity to perform this internship in collaboration with Lafarge and to gain experience with such a big variety of special measuring devices used in the building materials sector.

Following, special thanks to my Austrian Professor Dr. Harald Harmuth who prepared me greatly for this internship with all his passion and accuracy during the Master of "Building Materials" at the University of Leoben.

Further I would like to thank Stephane Rodts for his help and support concerning NMR measurement and mathematical analysis.

Moreover thank you to Francois Bertrand for his help during the MRI measurement, Laurent Tocquer for all his support and motivation, Nicolas Lenoir for the execution of the X-ray microtomography measurement, Roland Ramsch from Formulaction for the testing of the Turbiscan and Ian Haley and Benoit Faure for the presentation and testing of the FBRM® and PVM®.

Finally I would like to show my sincere thanks to my colleagues at Laboratory Navier for their friendliness and helpfulness and to my family in Austria for their general support.

Contents

List of abbreviations

$FBRM$	focused beam reflectance measurement
PVM	particle vision microscopy
MRI	magnetic resonance imaging
NMR	nuclear magnetic resonance
CCD	charge-coupled device
$T1$	spin- relaxation time
$T1$	Spin-lattice relaxation time
${}^1H$	hydrogen atom
rpm	revolutions per minute
$vol.\%$	volume fraction in percent
τ	shear stress
δ	deformation
γ	shear strain
$\dot{\gamma}$	shear rate
η	viscosity
G'	storage modulus
G''	loss modulus
$PIDS$	polarization intensity differential scattering
$ENPC$	Ecole nationale des ponts et chaussees
F	force
$\vec{S}$	magnetic spin
γ_1	gyromagnetic ratio
$\vec{m}$	magnetic dipole moment
$\|B_0\|$	applied magnetic field
ω_0	Lamor frequency
M_{xy}	magnetic moment in x-y plane
M_z	magnetic moment in z plane
$T0$	relaxation time of glucose-water mixture
$T1$	longitudinal spin relaxation time
$T2$	transversal spin relaxation time
I_0	conc. profile of the sample in initial state
I_1	conc. profile of the aged sample
Γ	torque

H	height of the inner cylinder
r	radius of the cylinder
v	velocity

1 Problem definition

1.1 Problem definition

Within the scope of the Master's thesis, a flocculation process in a model suspension should be analyzed. As a model suspension, calcium carbonat Durcal 5 mixed in different ratios with a mixture of 70 % glucose and 30 % water, was used. The characterisation of the flocculation process should be perfomed through describing the change in rheology within the time. For that purpose, the measurement of yield stress, loss modulus and storage modulus will be executed with the help of a rheometer and a magnetic resonance imaging device coupled with a rheometer.

The second goal is to link rheological properties with the state of flocculation concerning shape and size of flocs. For that reason, devices will be tested regarding their capability of direct flocculation observation in a dense opaque suspension. An important point is to distinguish between flocculation and the possible structure formation by bonding of flocs.

The data gathered during measurements, like size, shape and strength of flocs within the time, should give the necessary information for the planned numerical modelling of the flocculation process.

2 State of the art

Portland cement is the most important construction material in the world. Cement pastes and concrete structures obtained much attention by research in the last 50 years. Anyhow a great uncertainty remains still about phase formation in concrete and rheology of the paste.

The increase of fluidity helps to improve handling of a cement paste with a strong impact on final durability and strength of the concrete structure. Fluidity of the cement paste at early stage is expected to be strongly dependent on flocculation of fine particles in the paste and the start of cement hydration. The Master's thesis focuses mainly on the evaluation of different measurement devices capable to observe flocculation. Various optical devices like optical microscopy, confocal microscopy and others are tested. Additional information is gained by nuclear magnetic resonance measurements on the Bruker Minispec and magnetic resonance imaging. The results obtained by optical and magnetic resonance measurements are combined and compared with rheology properties.

2.1 Thixotropic fluids

Thixotropic fluids are non-Newtonian fluids. This means, that shear stress does not increase or decrease linearly with shear rate. In general speaking, the viscosity decreases due to the impact of mechanical force. In literature, a variety of definitions of thixotropy can be found.

The oxford Encyclopedic Dictionary of Physics gives the following definition

> "***Thixotropy:*** Certain materials behave as solids under very small applied stresses but under greater stresses become liquids. When the stresses are removed the material settles back into its original consistency. This property is particularly associated with certain colloids which form gels when left to stand but which become sols when stirred or shaken; due to a redistribtion of the solid phase[2]"

Lots of research was already done on thixotropic fluids, however it remains still a great uncertainty about the structure forming process and its influence on rheological

behavior of the fluid. Especially the rheological background of granular pastes is widely unknown but very important in cement industrie.

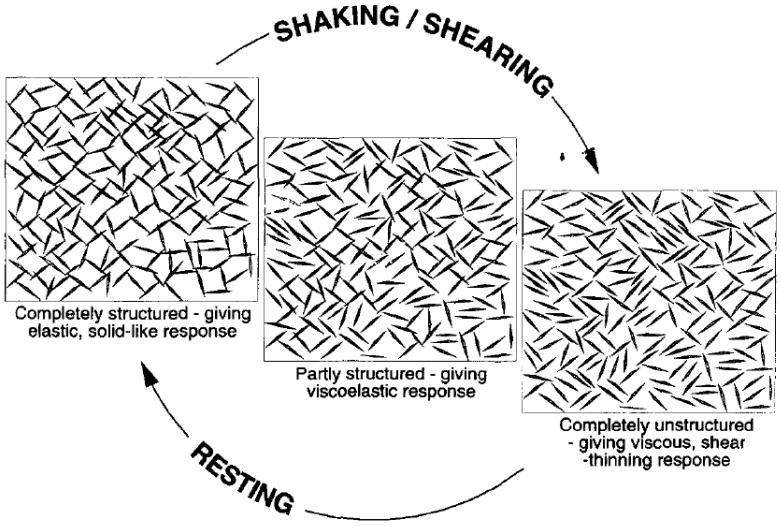

Figure 2.1: Breakdown of a 3D thixotropic structure [2]

.

Most suspensions (liquids mixed with solid particles) can show thixotropic behavior. A reason is the structure formation process in the suspension by flocculated solid particles during idle time. Idle time denotes a period of time without any mechanical impact on the suspension. Flocculation is caused by van der Waals forces, electrostatic or steric stabilization. The brownian motion leads to a movement to approach particles close enough one to each other. Brownian motion denotes the random thermal movement of atoms [2].

During the breakdown, some bondings in the structure are broken and the resulting particles or flocs are disordered. This process is completely reversible, which means, that a structure is again formed in the suspension and particles will find an equilibrium position after infinite time of rest. [2]

Granular pastes are still studied by research in three different approches:

1. the fluid rheology
2. the physics of granular matter
3. soil mechanics

In conclusion it is necessary to overlap the different strategies in this subject and combine them in a more general scientific approach.

2.2 Laboratory devices to characterize flocculation in dense opaque suspension

To follow flocculation of calcium carbonate Durcal 5 in a dense opaque suspension, the device has to be capable to measure a particle size range in between 1 μm and 100 μm. Additionally, results about change in concentration and rheology parameters like yield stress, storage modulus *G'* and loss modulus *G"* can give very useful information concerning flocculation. The following enumeration includes a state of the art overview of laboratory devices which could characterize flocculation including the comparisson of advantages and disadvantages of each of the devices.

2.2.1 Light microscopy

The light microscope is a laboratory device which uses a visible light source and a system of optical lenses to obtain a 2D-image of a certain sample area. The magnification is a product of different lenses and the resolution of the CDD-chip used. The light microscope works either in transition or reflection mode, where transmitted light or reflected light is detected.

Light microscopes have a few advantages which make them very competitive. First of all the low price in comparison to other laboratory devices and easy availability for measurements. Another important point is the magnification. The resolution of the light microscope is high enough to observe a particle size range in between 5 μm and several 100 μm. Further, form and porosity can be observed if the model suspension and the experimental execution is adapted. Moreover, results are not model based which is very important for the numerical modelling of flocculation.

The use of light microscopes at opaque suspensions has also some disadvantages. The sample can't be observed directly and without additional treatmant due to its opacity hence observation is limited to the surface.

2.2.2 Scanning electron microscopy

The scanning electron microscope uses an electron beam as a source instead visible light used at light microscopy. The electron beam scans the surface and highly increases the magnification of the microscope. It is capable to observe a nanometer lengthscale. The emitted light (from photons which can have a wavelength of visible light), high energy backscatterd electrons and X-rays contain information about the topography and the chemical composition of the sample surface. To avoid charging

effects at non-conductive materials, the sample surface has to be coated. The sample chamber itself is at partial vacuum.

The advantages of scanning electron microscopes are the very high resolution and the chemical analysis of the surface.

At suspensions, the scanning electron microscope has the disadvantage, that the partial vacuum in the sample chamber leads to fast evaporation of the liquid and causes therefore difficulties by drying at wet sample observation. Furthermore the disadvantages already pointed out at light microscopy are also valid at scanning electron microscopy.

Due to the micrometer lengthscale (located between 1 μm to 100 μm) of flocculation, the high magnification in the nanometer lengthscale of scanning electron microscopy has to be questioned.

2.2.3 Environmental scanning electron microscopy

The environmental scanning electron microscope applies an electron beam, equally to the scanning electron microscope, to scan the sample surface. The difference lies in the environment in the sample chamber. Instead a partial vacuum used in the scanning electron microscope, the environmental microscope uses water vapour, nitrogen or air as imaging gas atmosphere. Due to the application of water vapour, a costly coating can be avoided, because non-conductive samples are discharged over the gas phase. Additionally, the sample liquid doesn't vaporize due to the water vapour partial pressure.

The environmental scanning electron microscope has the advantage of elimintation of drying during measurement by the water vapour partial pressure in the sample chamber but has difficulties to obtain high resolutions at very wet samples [13].

2.2.4 Soft x-ray transmission microscopy

At soft X-ray microscopy, soft X-rays are used as radiation source. The resolution of a X-ray microscope is in between the resolution of a light and an electron microscope. As radiation source, a Synchrotron with a plane mirror, can be used. A synchrotron is a circular particle accelerator where radiation is emitted as a by-product [15]. The plane mirror enables the passage of the soft X-ray range. Afterwards, the soft X-ray beam is focused by a condenser plate on the sample. After transition of the sample, the beam is refocused and detected by a X-ray CCD-chip. The maximum resolution is around 25 nm [13]. A sample diameter is limited to 10 μm.

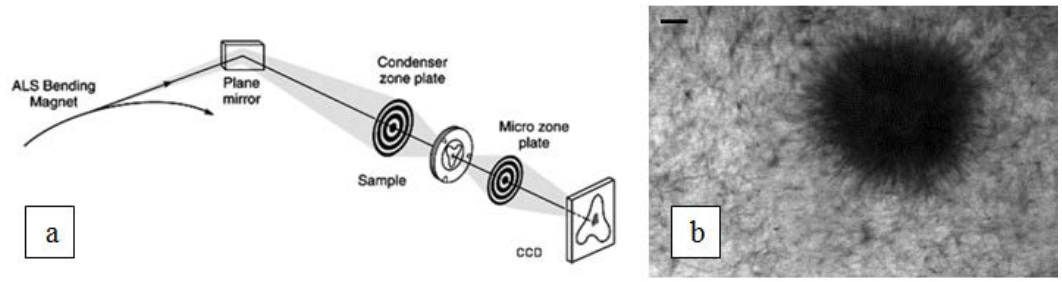

Figure 2.2: a) Soft X-ray transmission microscopy b) Tricalcium silicate in solution saturated with $Ca(OH)_2$ and $CaSO_4 \cdot 2H_2O$, scalebar = 1 μm [13]

Its high resolution and the ability to measure wet samples at ambient pressure can be pointed out as advantages.

A disadvantage of the soft X-ray transmission microscope is the small sample diameter of 10 μm, which reduces the usability at bigger particle size fractions, according to Juenger [13]. Moreover, the availability is strongly limited due to the difficult accessibility of a Synchrotron radiation source.

2.2.5 Confocal microscopy

The confocal microscope is a light based microscope. Usually water or oil lenses are used to improve the image quality. It has the ability to focus the depth of a sample more precisely. This leads to a higher resolution in the profundity of a sample and helps to create 3D-models of transparent suspensions. This advantage is achieved by point illumination of the sample and by the use of a pinhole to eliminate not focused light. The image is build up by point to point illumination.

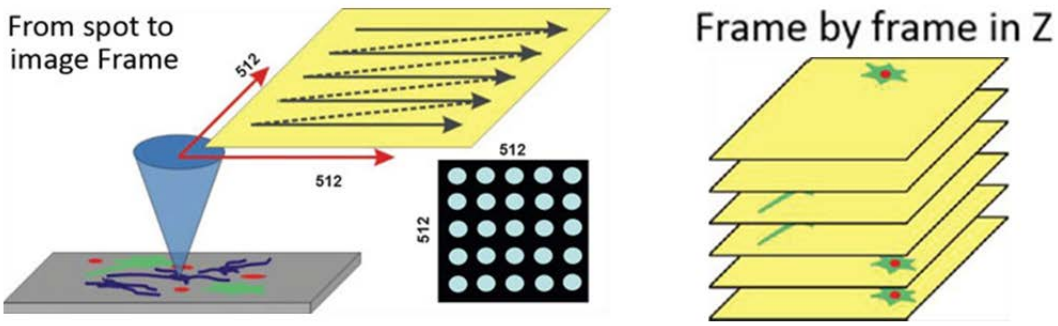

Figure 2.3: Point-scanning LSCM: functionality of confocal microscopy [12]

Due to the detection of reflected light, the sample can be directly observed. Bromely [5] points out, that further advantages lie in its high spatial resolution and relatively

short aquisition time. Anyhow, the observation depth in dense opaque suspensions is limited to several micrometer and therefore not representative. Furthermore a solvent needs to be used to have a close refractive index match in between the liquid and the solid particles.

2.2.6 Atomic force microscopy

The AFM - "Atomic force microscope" consists of a soft cantilever with a thin tip. This thin tip is moved by a mechanical scanning system (piezoelectric) close to the sample surface. The soft cantilever and thin tip are sensitive to surface forces. The surface attraction is composed of van der Waals forces, chemical bonding and electrostatic forces. The deflection is usually measured by a laser beam and is directly passed to a feedback system to analyse the data [24]. The optical detection devices can measure deflections down to 0.1 Å, which makes it one of the most sensitive measuring devices available.

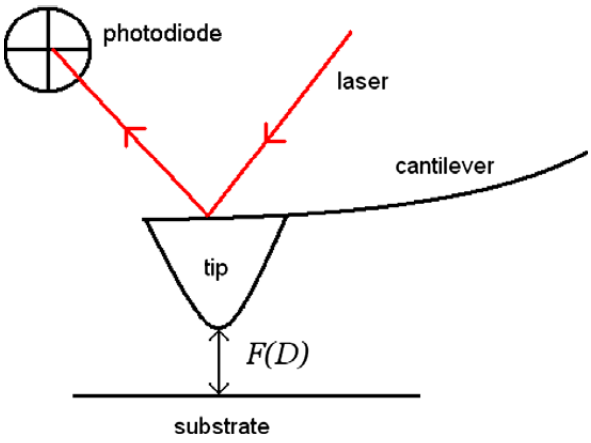

Figure 2.4: AFM setup [7]

According to Ferrari [7], AFM requires well-defined, flat and non-reactive substrates.

The advantages for the use of the AFM are the suitability for wet samples and its very high resolution.

The vertical distance resolution of a nanometer lengthscale is too small to deliver meaningful data about flocculation. Furthermore, a measurement accuracy of 0.1 Åis too exact for flocculation observation. It also doesn't allow volumic observation, observation of structure, porosity and is further not available in the laboratory.

2.2.7 Laser diffraction particle size analyzer

The laser diffraction particle size analyzer is a light diffraction particle size analyzer. It is composed of a dilution and a measurement unit. The dilution unit is a water cup where the sample is diluted in water until a certain concentration. Then the very thin suspension is pumped in circle and passes a laser beam. The laser beam illuminates the sample and is diffracted in various directions. Large particles scatter light at small angles relative to the laser beam and small particles scatter light at large angles [19]. The diffracted light is detected by several detectors around the sample. The detection unit is composed of various back scattered light detectors, large angle detectors and a focal plane detector. The measureable particle size range is in between 100 nm and 3.5 mm.

The laser diffraction analyzer has the advantage, that the measurement is very fast. Further, it can be used for opaque suspensions due to the dilution of the sample. On the other hand, the analysis is very sensitive to particle shape. The software calculates the resulting spheric diameter for a certain particle size measured, which is a rough approach. Concerning the observation of flocculation, the pumping of the suspension can have a strong impact on flocs and can possibly destroy them.

2.2.8 FBRM® - "Focused beam reflectance measurement"

FBRM® - "Focused beam reflectance measurement" is a measuring device for in-time and in-situ particle size measurement. According to Blanco [4], a focused laser beam is rotating with a fixed speed, scanning across particles. A detector measures the time of reflection of one particle. The time of reflection multiplied by the velocity of rotation of the laser results in the strongly particle shape dependent "chord length".

A huge number of "chord lengths" needs to be measured to reduce the statistical failure of the particle size distribution. The device measures in a particle size range of 500 nm to 3 mm. The upper limit is due to the laser aperture of the FBRM® device.

Due to the reflection light detection of the FBRM®, the FBRM® can be used in dense opaque suspensions. Another advantage is the very short measurement time which makes it possible to follow directly a structure formation process in a sample. To improve the reliability of the particle size distribution and the statistical correctness, a minimum measurement time is essential.

The difficult accessibility, the model dependency and the high price can be stated as disadvantages. Moreover, short distances in between particles due to high vol-

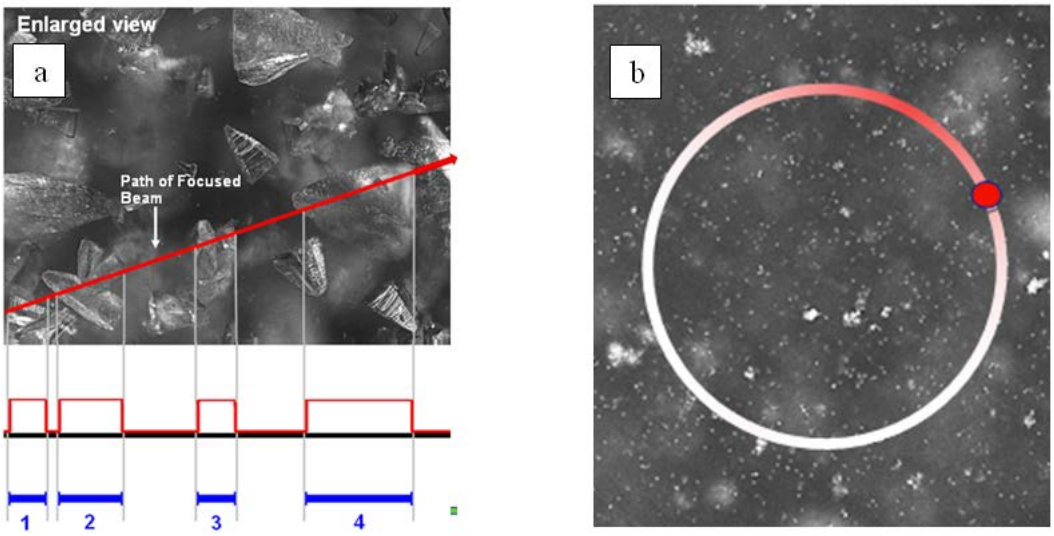

Figure 2.5: a) Path of focused beam during FBRM® measurement. b) View from FBRM® probe window illustrated in PVM® image [10].

ume fractions lead to measurement problems in macro and micro mode. Further information concerning this problem can be found in section 4.5.

2.2.9 PVM® - "Particle vision microscopy"

The "Particle vision microscopy" is an optical measurement device which measures in real time. The PVM® consists of a light source and a high resolution CCD-camera. The software iC FBRM allows the analysis of the raw data to improve the understanding of the particle systems.

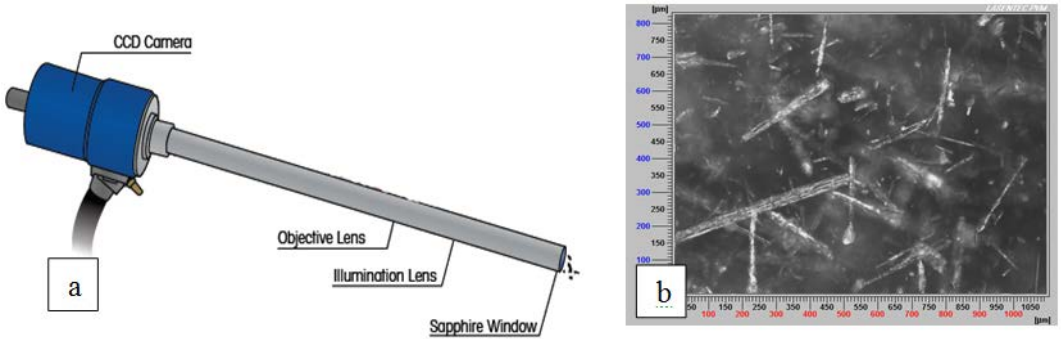

Figure 2.6: a)PVM® measurement unit b) PVM® image [10]

The PVM® has the advantage of direct observation due to the light source and the high resolution CCD-camera. A disadvantage is the high price. The analyses is more efficient concerning particle size measurement in connection with a FBRM® by the

direct measurement of the particle size distribution. Additionally there are doubts about the suitablity to measure very dense opaque suspensions.

2.2.10 Turbiscan - "Static multiple light scattering"

The Turbiscan is an optical table measurement device. It does observe change of average size and concentration [8] and therefore the dispersion state of the suspensions. The Turbiscan is based on the principle of multiple light scattering. The sample is illuminated by a laser light source, then the light is scattered many times in the sample itself before it emerges back to the sample surface where it is detected by a measurement device. The sample itself is put in a glas cell. The particle size range is in between 10 nm and 1 mm.

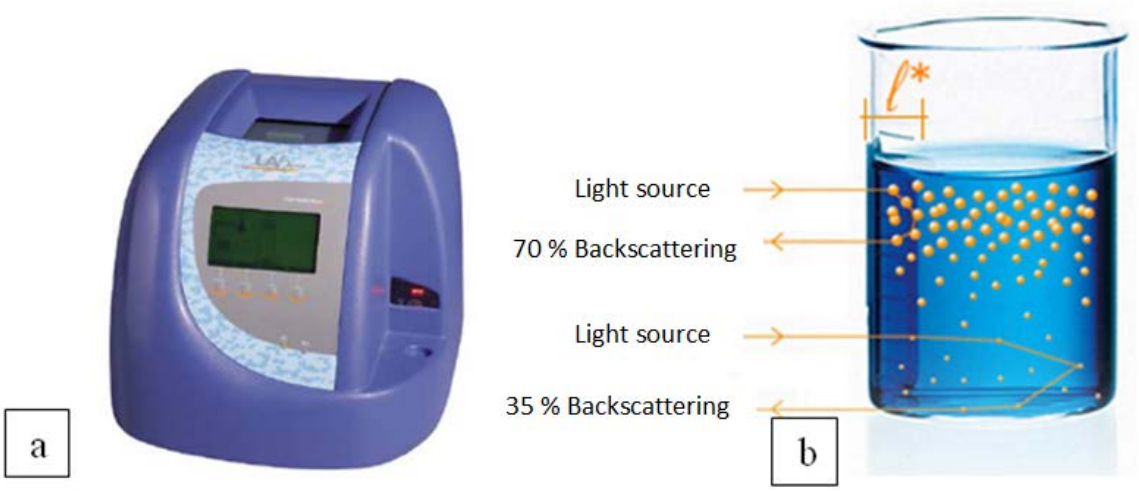

Figure 2.7: a) Turbiscan: Measurement of instability phenomena. b) Measurement principle of the "Turbiscan" by multiple light scattering [8].

An advantage of the Turbiscan measurement is the very fast and non-contact measurement. As a disadvantage can be stated, that it is only possible to follow the evolution of the average particle size instead real evolution of particle size distribution. A further disadvantage is the strong model dependency which makes it difficult to use the results as a bases for a scientific model.

2.2.11 SAXS - "Small angle X-ray scattering"

The SAXS uses a X-ray radiation for measurements. X-ray radiation has a wavelength between 10^{-8} m and 10^{-12} m. Therefore it lies in between gamma and ultraviolet light. If a X-ray beam passes through a sample, a small portion of the beam is

scattered out of the beam in a small angle due to heterogenities. At laboratory devices, either a rotating anode source or a sealed tube source can be used. To improve the brilliance of the X-ray beam, a synchrotron light source can be used.

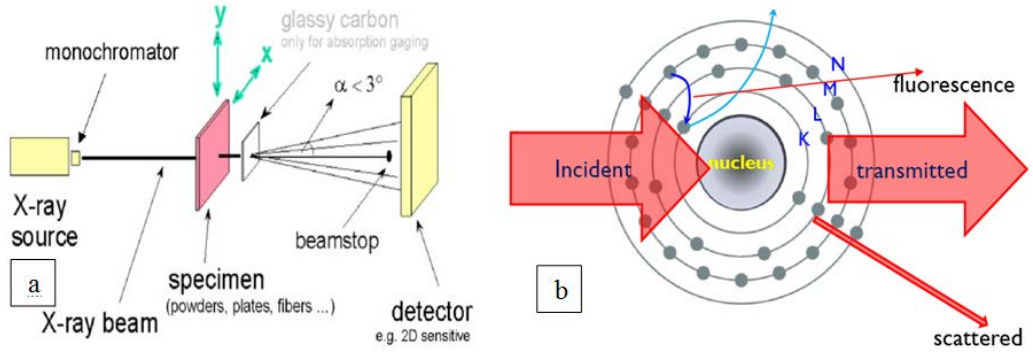

Figure 2.8: a) SAXS: measurement setup [6] b)Measurement principle of the SAXS by small angle X-ray scattering [25].

Allen [1] points out, that the angular profile of the small-angle scattered intensity is effectively a Fourier transform of its microstructure. It can be analyzed to obtain the statistically representative partical size distribution. The data is based on a microstructure model which is determined by the measured parameters. Particles with a size over 25 nm can be observed. It can give information about particle shape, size and pore structure of macromolecules with a resolution higher than 25 nm.

The SAXS has thus the great advantage, that it gives information about particle shape and pore structure. Furthermore it is a very precise measurement tool.

The disadvantages are again the strong model dependency, the high price and the very complex data evaluation. If a synchrotron light source is used, the restricted accessability also has to be pointed out.

The SANS - ”Small angle neutron scattering” is quoted additionally and is in many aspects similar to the SAXS measurements.

2.2.12 X-ray microtomography

According to Lenoir [17], tomography techniques are:

> "Non destructive methods which allow studying composition and internal structure of bulk objects."

The X-ray microtomography is a 3D-characterizing non-destructive measurement device. According to Landis [16], the X-ray microtomography can obtain a resolution smaller than 1 μm. It maps the attenuation of X-ray radiation in a sample which is closely related to the density [14]. The radiation source is either a Synchrotron or a X-ray tube source. The light from a synchrotron source is brigther and gives a higher contrast and brilliance, which helps to distinguish very subtle changes in materials. The sample is rotated during measurement. The aquisation time depends on the properties of the sample itself and can last up to three hours. Due to the measurement, two-dimensional images called slices are created and can be reconstructed by analytical methods.

An advantage of the X-ray microtomographe is the non-destructive resolution in the micrometer size range which can be used for 3D-imaging.

Disadvantages are the long aquisation time, which can lead to problems in less stable suspensions and the big amount of data obtained (8 GB for a high resolution image). The light source used in the laboratory has the disadvantage of very long aquisation time, the fast measurement of the synchrotron on the other side is only very difficult available.

2.2.13 Minispec

The Minispec is a Nuclear magnetic resonance table device from BRUKER to measure magnetic relaxation time of hydrogen nuclei ^{1}H in the sample after excitation. The measurement of ^{1}H relaxation is most frequently used due to the presents of hydrogen in most samples. Also other elements can be measured by a change in setup. The sample size depends on the testing probe used and varies from an external diameter of 1 cm up to 1.8 cm. During insertion of the sample in the Minispec, the hydrogen nuclei are aligned according to the principal magnetic field of the device. A radio frequence antenna excites the hydrogen nuclei ^{1}H. When the excitation is stopped, the time of relaxation is measured by the radio antenna.

Two common measurement modes exist which are usually used to measure magnetic relaxation. First T1 (Spin-lattice relaxation time) is the back alignment of the magnetic vector from the excitation position to the main magnetic field. Second T2 (Spin-Spin relaxation time) denominates the relaxation of the hydrogen magnetic vector in the x - y plain. The T2 relaxation time is shorter and as maximum as long as T1.

The particle concentration in the sample is dependent on relaxation time, due to the coherence of relaxation time velocity to surface proximity. In general it can be pointed out, that regions with less particle concentration relax slower and regions

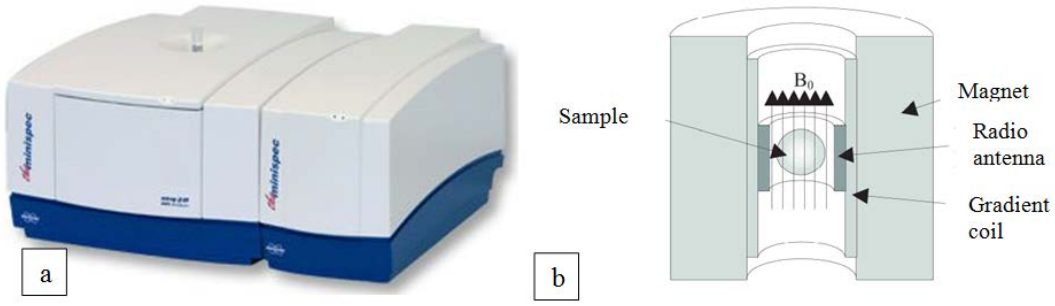

Figure 2.9: a)Bruker Minispec: NMR table device. b) NMR setup in the Bruker Minispec [23].

with more dense concentration relax faster. This can give information about progress in inhomogenity caused by flocculation or structure formation.

The minispec has the advantage to measure very small sample sizes (2 ml - 6 ml) and to follow the evolution process in a sample over a few days.

Disadvantages are the complicated data analysis/interpretation and the link with sample evolution and sample properties.

2.2.14 MRI - Magnetic resonance imaging coupled with a rheometer

The magnetic resonance imaging device is a laboratory NMR device coupled with a rheometer. The alignment of ^{1}H nuclei and the excitation is based on the same principle as the Minispec. The magnetic coil is bigger due to the necessity to obtain a very homogenous principal magnetic field for a sample size of around one liter with a diameter of about 12 cm. A magnetic field gradient is used to gain information about the area of measurement.

The MRI device allows the measurement of the velocity gradient during stirrer movement in the annular gap between the inner and the external cylinder in the rheometer. The resolution of the magnetic resonance measurement is around 1 mm. Further information can be obtained about local density.

The advantage of MRI is the coupling of magnetic resonance with a rheometer measurement. This gives very important information about rheology properties and at the same time the velocity gradient and density distribution in the sample.

Disadvantages are a resolution of about 1 mm, the very expensive testing conditions due to high operating costs and the availability.

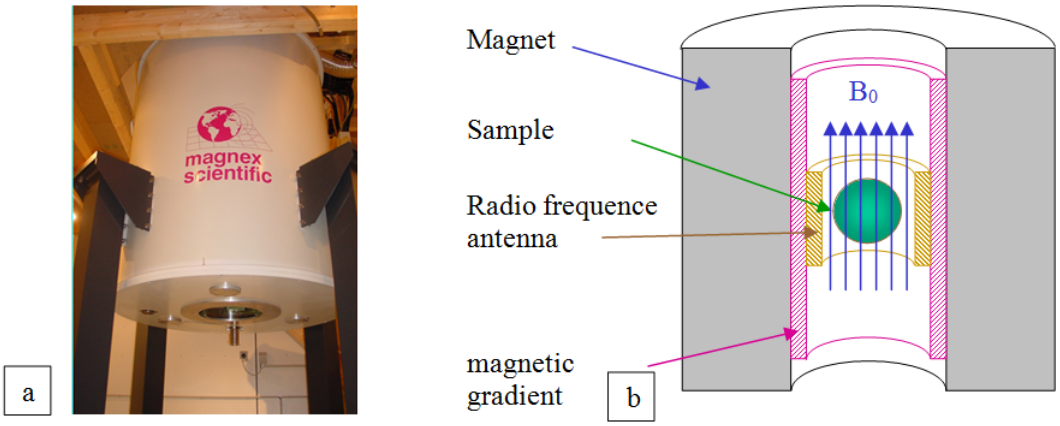

Figure 2.10: a) MRI coupled with a rheometer at "Laboratoire Navier" b) Setup of the MRI device [23].

2.3 Rheometry

Rheology describes the behavior of deformation and stress in fluids. It is called fluid mechanics.

$$\tau = \frac{F}{A} \tag{2.1}$$

As valid in solids mechanics, shear stress is equal to force per surface.

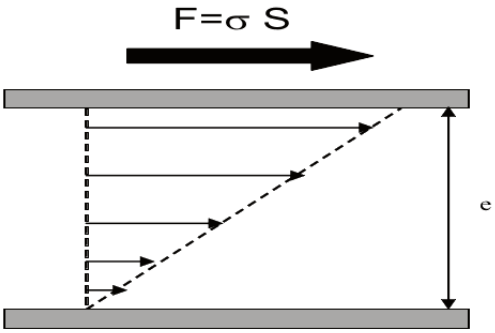

Figure 2.11: The measurement principle of rheology experiments. The sample is inserted in between to plane surfaces S, with a distance e. A constant force F= σ S is applied at the upper plane. The deformation of the suspension δ is measured.

The ratio of deformation δ to the certain distance between two plane surfaces e is called shear strain γ.

$$\gamma = \frac{\delta}{e} \tag{2.2}$$

The shear rate (equation 4.3) is the ratio of velocity and the distance between a static and a moving surface.

$$\dot{\gamma} = \frac{dv}{de} \tag{2.3}$$

Two extrems have to be considered:

In the Newtonian case, the plane is moving with a constant velocity, the viscosity is the resistance of the fluid against flow. It is defined by:

$$\eta = \frac{\sigma}{\dot{\gamma}} \tag{2.4}$$

The energy is dissipated.

In the second case, the total energy is stored elastically which is called a Hookean-solid. If force is applied, the solid will be deformed. Shear strain is again deformation δ divided by distance e.

$$\gamma = \frac{\delta}{e} \tag{2.5}$$

If a complete turn of 360° of the rheometer is considered, differences in phase between two phase angles can be determined. Solid materials show a direct relation between strain and phase angles, therefore the phase angle is 0. Liquids have an invers behavior. If the strain rate is at maximum, the change in stress will be at a minimum or zero with a phase angle of 90°. In practice, materials have phase angles in between 0° and 90°.

$$\sigma(t) = \sigma_0 cos(\omega t) cos(\phi) - \sigma_0 sin(\omega t) sin(\phi) \tag{2.6}$$

To distinguish between elastic and viscous components, the storage modulus G' and the loss modulus G'' can be measured.

$$G'(\omega) = \frac{\sigma_0}{\gamma_0} cos(\phi(\omega)) \tag{2.7}$$

$$G''(\omega) = \frac{\sigma_0}{\gamma_0} sin(\phi(\omega)) \tag{2.8}$$

The name storage modulus is derived from the storage of energy due to the elastic reversible properties. The name loss modulus comes from the loss of energy through permanent deformation caused by viscous properties. The behavior in between is called viscoelasticity.

2.3.1 Liquids with Yield stress

Many materials in civil engineering are concentrated suspensions of liquids mixed with solid particles of different size and shape. At weak stress or small deformations, the suspension acts elastically like a solid. Above the yield stress, the properties of the suspension are like a viscous fluid.

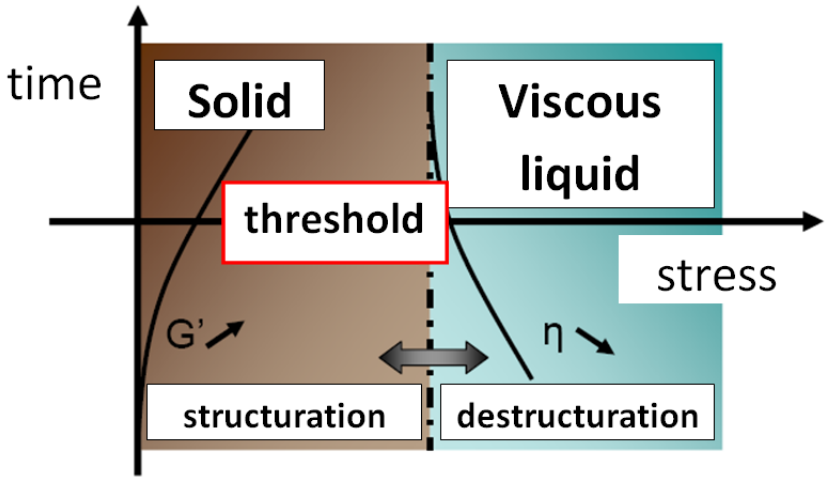

Figure 2.12: Properties of a suspension with yiel stress according to [9].

To measure the yield stress, a small deformation is applied and the evolution of stress σ with time is measured until reaching a plateau.

2.4 Magnetic resonance

The magnetic resonance devices in the laboratory of the research group Navier work with ^{1}H excitement. The magnetic spins $\vec{S}$ are aligned by a main magnetic field of 0.5 T. The main magnetic field is created at the MRI by a magnetic coil and at the Minispec by a permanent magnet.

The resulting magnetic moment is calculated by:

$$\vec{m} = \gamma_1 \vec{S} \tag{2.9}$$

Gamma γ_1 denotes the gyromagnetic ratio which corresponds to the ratio of the magnetic dipole moment $\vec{m}$ to the angular moment with a value of 2.675*10^8 rad s^{-1} T^{-1}.

Without the main magnetic field, the magnetic spins are randomly orientated to reach a state of lowest energy potential, thus spins eliminate each other. If a magnetic field is present, the magnetic spins $\vec{S}$ are aligned along the magnetic field.

$$\omega_0 = \gamma_1 |B_0| \tag{2.10}$$

The gyromagnetic ratio γ_1 multiplied with the magnetic field $|B_0|$ results in the Larmor frequency ω_0. The Larmor frequency describes the pricession of the magnetic moment about an external magnetic field.

The magnetic moment is composed of a magnetic moment M_{xy} in the x-y plane and a magnetic moment M_z in z direction. The radio antenna excites the magnetic spins and aligns them in another direction, different to the main magnetic field. The excitation is biggest, if the excitation frequence corresponds to ω_0, the Lamor frequence. After excitation, the relaxation time of the magnetic spin is measured by the radio antenna. The longitudinal spin relaxation time or relaxation in z direction is called T1. The transversal spin relaxation time or relaxation in x-y plane is called T2.

3 Materials

3.1 Materials

Portlandcement mixed with water forms a highly reactive suspension. To avoid the influence of hydration on early paste properties and to assure to measure only a flocculation process, a mixture of $CaCO_3$, Glucose and water is used as a model material. To obtain samples with a stability up to at least 24 hours, water is mixed with glucose to increase viscosity and to avoid sedimentation.

3.1.1 Calcium carbonate $CaCO_3$

Durcal 5 from Omya is calcium carbonate from a natural resource. It is used as an inert filler in cement industrie, in paint and varnish. It has a high whiteness and a 98 % chemical purity. Minore mineral phases are 1.5 % of $MgCO_3$, 0.03 % of Fe_2O_3 and 0.3% of insolubles HCl. Further trace elements occure like cadmium, lead, manganese and copper. Due to its inert properties, it is a perfect material to study impact of flocculation by excluding rheology change caused by hydration. The content of impurities is important due to the impact of alkali introduction and following improvement of flocculation.

The avarage particle size is 4.5 μm with a specific surface of 21000 cm^2/g. The solid density is 2.7 g/cm^3.

The particle shape is not spheric and formed by crushing and milling.

3.1.2 Water

Purified water is used for sample preparation. This is important to avoid the introduction of additional ions which can influence flocculation. The water is put in a beaker and heated up until a temperatur of at least 60°C. Than water is mixed in a certain amount with glucose.

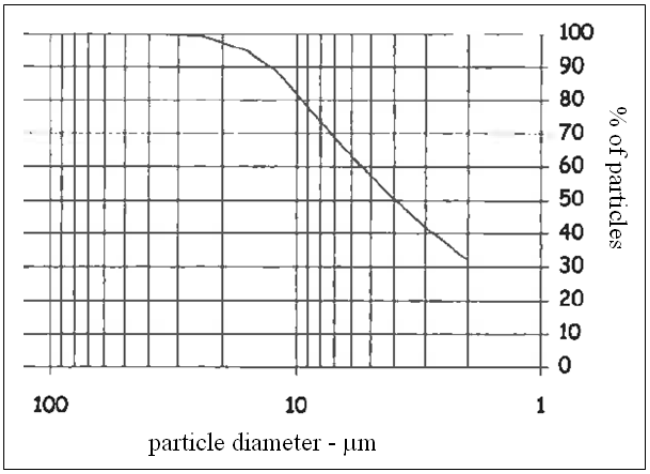

Figure 3.1: Particle size distribution of Durcal 5.

3.1.3 Glucose

Glucose is a simple monosaccharide which is produced in plants during photosynthesis. The velocity of solubility of glucose in water is improved by the increase of temperature. By heating up to 60°C, solubility of glucose is increased. Glucose molecules form circles which can be broken up in small quantities during dilution in water, forming open chains.

The testing is performed with glucose sirup 5 NA of Nigay. Glucose sirup 5NA indicates, that it is a mixture of water and glucose. The glucose sirup is mixed with 30% of water to obtain concentrations of 70% glucose sirup and 30% water. Glucose is used to improve viscosity and to reduce particle sedimentation in the sample.

3.1.4 Glucose-water mixture

A glucose-water mixture was used to avoid the influence of sedimentation and to obtain stable testing conditions for at least 24 hours. Different mixing rations of glucose-water mixture were tested concerning sedimentation. An optimum was found at 70% glucose and 30% of purified water. This mixture was used for all test runs. Glucose and water were independently heated until 60 °C and mixed until the whole glucose was solved in water.

3.1.5 Glenium

Is a water reducing admixture (dispersant) from BASF used in concrete paste. The dispersion effect is caused by polycarboxylate [3]. It is used to improve consistency

and flowability of concrete paste, at self-consolidation concrete and concrete with various water reduction requirements. The amount of admixture is variable until a maximum of 1.8 % of solid weight. Glenium has to be stored above 5 °C.

4 Testing Devices and Methods

The devices quoted in chapter 4 were tested on the calcium carbonat model system. The majority of devices was available at Ecole des Ponts ParisTech and further tests had been performed with industrial partners like ”Mettler-Toledo” or ”Formulaction”.

4.1 Transmitted light microscopy

The Zeiss transmitted light microscope is based on visible light. A Zeiss Axio Observer A.1 was used.

4.1.1 Test execution

With help of the transmitted light microscope, a sample with 47 vol.% Durcal 5 mixed with the glucose-water mixture was observed at fresh state, after 24 hours, after 24 hours with 1.8 % of Glenium and after one week of preparation (each time newly prepared). For sample preparation, Durcal 5 was mixed with the glucose-water liquid for 1 minute with a Heidolph mixer at 400 rpm.

A tip of the suspension was put on a sample holder by a spatula. Further it was diluted with a drop of purified water and fixed with a cover slip. Due to the movement of the cover slip, the suspension drop was mixed with the purified water and formed a monolayer on the edge of the suspension drop. This monolayer could be observed at the transmitted light microscope.

4.1.2 Results

Figure 4.1 on the next page shows the results obtained by the transmitted light microscope. The suspension is diluted with water and forms, caused by the pressure of the cover slip on top, a mono or at flocs a thin multilayer of calcium carbonate particles.

Figure 4.1 a shows the influence of Glenium on flocculation. The particles are perfectly dispersed and formed no flocs. In the microscope, a movement of the particles

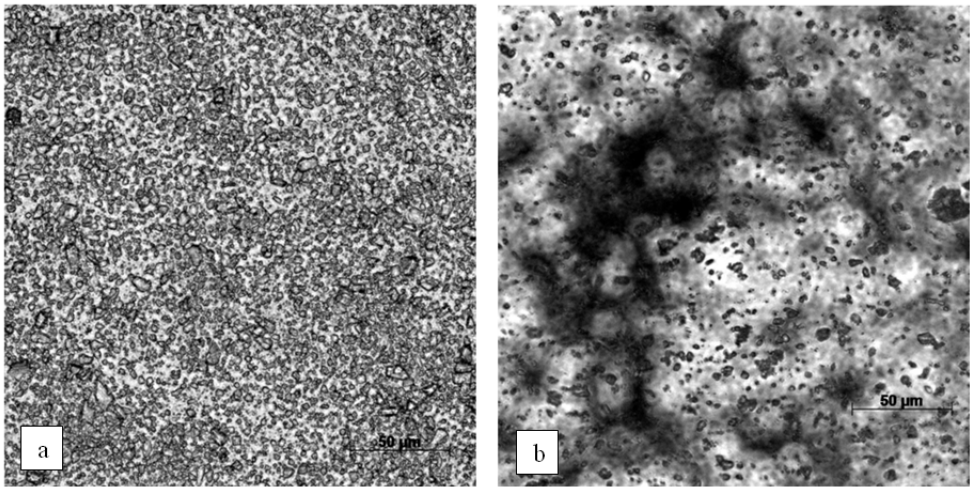

Figure 4.1: a) Suspension with 47 vol.% Durcal 5 and the glucose-water mixture with 1.8% Glenium after one week of preparation. b) Suspension with 47 vol.% Durcal 5 and the glucose-water mixture after one week of preparation.

due to repulsion forces caused by the dispersant was visible. Figure 4.1 b shows the formation of a floc structure due to coagulation of calcium carbonate particles. The formed flocs have a particle size of up to 150 μm, which corresponds to 30 times the average particle size of Durcal 5.

4.1.3 Conclusion

The testing at the transmitted light microscope demonstrates, that the observation of an opaque suspension is possible, if the suspension is diluted and is present in a monolayer or thin multilayer. It doesn't correspond to a direct observation of the sample. The picture gives qualitative information about floc structure and state of flocculation with no quantitative information for analysis and subsequent numerical modelling. Further it must be pointed out, that the impact on flocs by dilution and the pressure by the cover slip can break up floc structure.

4.2 Confocal microscopy

The testing was performed at Agro ParisTech. A Leica Inverted Fluorescent Microscope (Leica DMIRE2) with a water optical lense was used.

The apparatus of the confocal microscope is equipped with two motors which can move the top and bottom plane independently. This helps to investigate the influence of stress on structure and flocs.

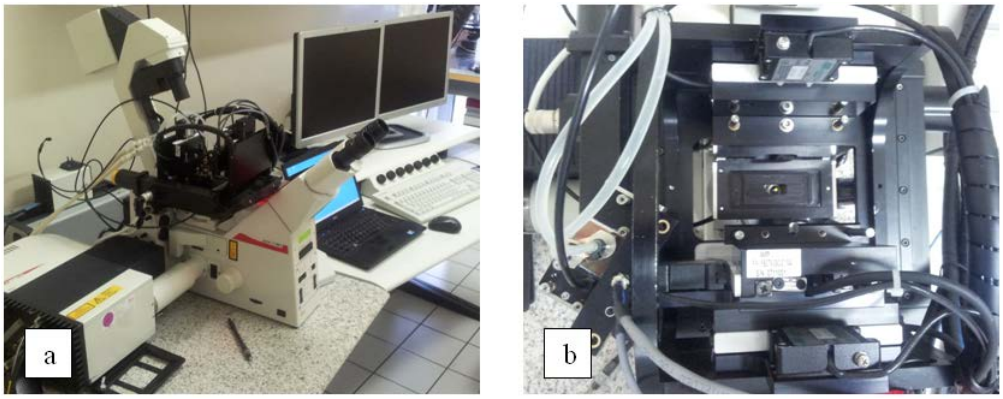

Figure 4.2: a) Leica "DMIRE2 Confocal Microscope" at AgroParisTech b) The apparatus with the optical lens in the center and the sample holder.

4.2.1 Test execution

A suspension of 42 vol.% and 47 vol.% of Durcal 5 with and without Glenium was tested. First, the glucose-water liquid was mixed with Fluorescein from Fluka. Fluorescent contrast agents are used to optimize imaging. Following, the liquid was mixed with Durcal 5 and stored for 24 hours to leave enough time for flocculation and structure formation.

At the confocal microscope, the suspension was put on a sample holder and was covert by a plastic plate, fixed on the movable installation of the apparatus. For the observation, the TxRed filter has been used. The testing was performed with certain speed of the bottom and the top plane to observe the impact of stress on particles.

4.2.2 Results

The suspension was directly observed by the confocal microscope. The observation depth amounted to several micrometer. Due to the average particle size of 5 μm and the size of flocs of up to 150 μm, direct observation of the upper layer of the suspension was not representative and not revealing.

Figure 4.3 shows dark regions with different size, which represent flocs and red regions of the water-glucose-Fluorescein mixture.

4.2.3 Conclusion

The confocal microscope is not suitable for direct observation of dense opaque suspensions due to the very low observation depth of several micrometer. An exact quantitative dilution of the suspension without a very strong impact on flocs at

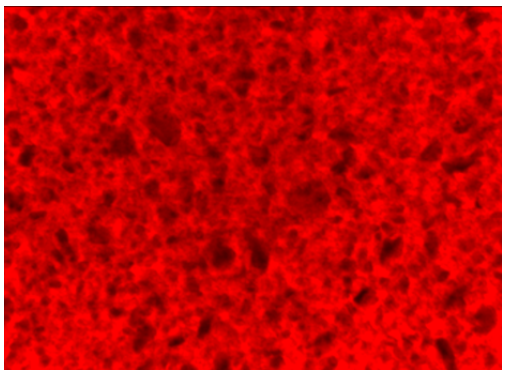

Figure 4.3: Suspension with 42 vol.% Durcal 5 observed by a confocal microscope.

different time of rest could improve observation but has the problem of change in structure and quantitative composition.

4.3 Turbiscan

The measurement principle of the Turbiscan is based on multiple light scattering. According to Formulaction [8], it is a measurement device used as a reference for stability analysis.

The testing was executed by a TurbiscanLAB with a diode light source emitting light with a wavelength of 880 nm and two photodiodes which measure the emerging light at an angle of 135°.

4.3.1 Test execution

A first sample was send to Formulaction in a mixed state at the beginning of the internship, therefore it was send with a 40 vol.% Durcal 5. The sample was mixed at 1600 rpm for 5 minutes to break up floc structure. The measurement was started directly after mixing.

The second sample was send in an unmixed state and prepared directly in the laboratory, also with a volume fraction of 40 vol.% to be able to compare results.

For each sample, every 30 seconds within the first 30 minutes and following, every 5 minutes a measurement was done.

4.3.2 Results

Figure 4.4 shows the results for the already flocculated sample after 5 minutes of mixing at 1600 rpm to destroy floc structure. It demonstrates, that the intensity of the backscattering signal doesn't change, which indicates usually stable samples.

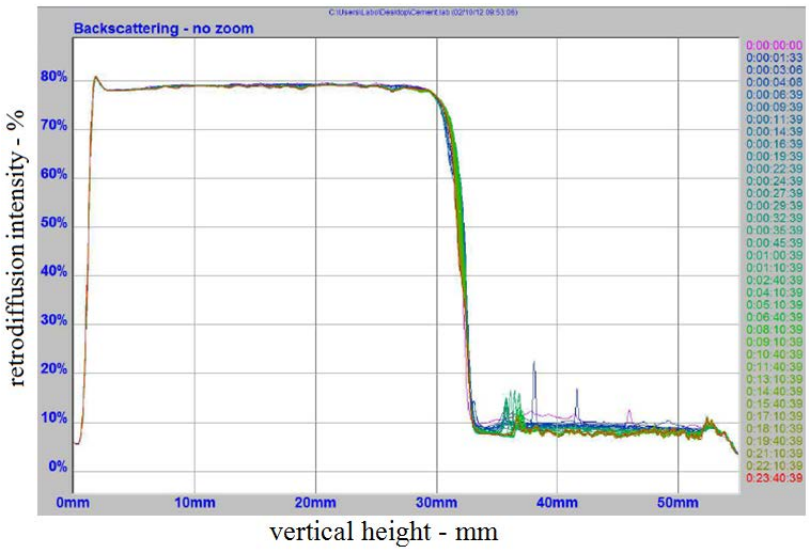

Figure 4.4: Turbiscan backscattering measurement of a suspension with 40 vol.% Durcal 5 with the glucose-water mixture.

The second graph shows the evolution of the backscattering signal which decreases 0.3 %. This demonstrates, that a non-significant evolution takes place.

Figure 4.5: Evolution of the backscattering signal with time at a suspension of 40 vol.% Durcal 5 and the glucose-water mixture.

Moreover, the calculation of the size of diffusers depend on the refraction index of the solvent and the particles. For the glucose-water mixture, a refraction index of 1.40 - 1.42 was choosen. For calcium carbonate, a standard refraction index of 1.59 was used and a particle size of 3.178 μm to 5.78 μm could be measured. Further it has to be pointed out, that the sample sent in mixed state and the sample sent separatly and mixed later, obtained the same results.

4.3.3 Conclusion

The Turbiscan doesn't measure a significant evolution in the sample. This can be explained by the small movement of particles necessary to flocculate in a supension with very high volume fraction of solids.

The Turbiscan is a very efficient device to measure stability of a suspension but doesn't provide useable data for numerical modelling of flocculation due to the output of an average particle size and not a particle size distribution.

4.4 Laser diffraction particle size analyser

According to 2.3.7, the laser diffraction particle size analyser is a measuring device to analyse the particle size of a suspension diluted in a liquid due to laser diffraction and laser diffusion.

4.4.1 Laser diffraction particle size analyser used in the Laboratory

The testing was performed with a "Granulometre laser LS230" from Beckman-Coulter. It allows a particle size measurement within a range of 0.4 μm - 2 mm. The suspension is inserted in water, which is used as testing liquid. At a certain concentration, which is measured and indicated directly by the laser diffraction analyser, the testing is started. A pump circulates the liquid to the measuring devices. The "Granulometre laser LS230" has a special feature for particles smaller than 1 μm, which is called "PIDS". "PIDS" stands for "Polarization Intensity Differential Scattering". It extends the measurement range from 0.1 μm to 0.4 μm.

4.4.2 Test execution

At the Laser diffraction particle size analyser, suspensions with 42 vol.%, 45 vol.%, 47 vol.% and a sample with 45 vol.% Durcal 5 and 1.8 % Glenium mixed with the

glucose-water mixture, were tested. The samples were prepared one day in advance to observe the sample in a flucculated state.

The suspension was inserted in the laser granulometer by a spatula and diluted in water until a certain concentration. Following, the water with the suspension was circulated by a pump to the measuring device. Due to the impact of the pump force on the floc structure, the pump speed was changed to observe its influence.

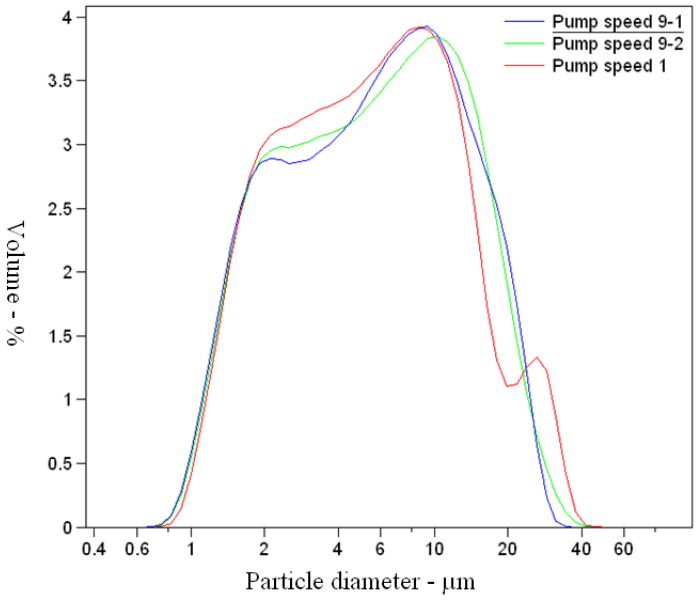

Figure 4.6: Suspension with 47 vol.% Durcal 5 and the glucose-water mixture at a flocculation state of 24 hours tested at different pump speed.

The pump speed showed a small influence at a particle size range of 10 μm to 30 μm, caused by a possible break down of flocs.

Two explanations can be pointed out, either even at the smallest pump speed, flocs are broken and the difference can be attributed to a measurement deviation or the structure is strong enough and is only partly broken by pumping.

4.4.3 Results

The results in figure 4.7 show a flocculation state after 24 hours of idle time.

The sample containing the dispersant Glenium, which delays or prevents flocculation, a maximum particle size, in between 10 μm and 20 μm with a peak at 9 μm, was measured. This corresponds roughly to the particle size distribution of Durcal 5 powder. At a volume fraction of 42 % Durcal 5, the maximum particle size increases to 25 μm. A particle size of 25 μm can't still be pointed out as a consequence of flocculation, due to the particle size cut at 24 μm at the Durcal 5 powder.

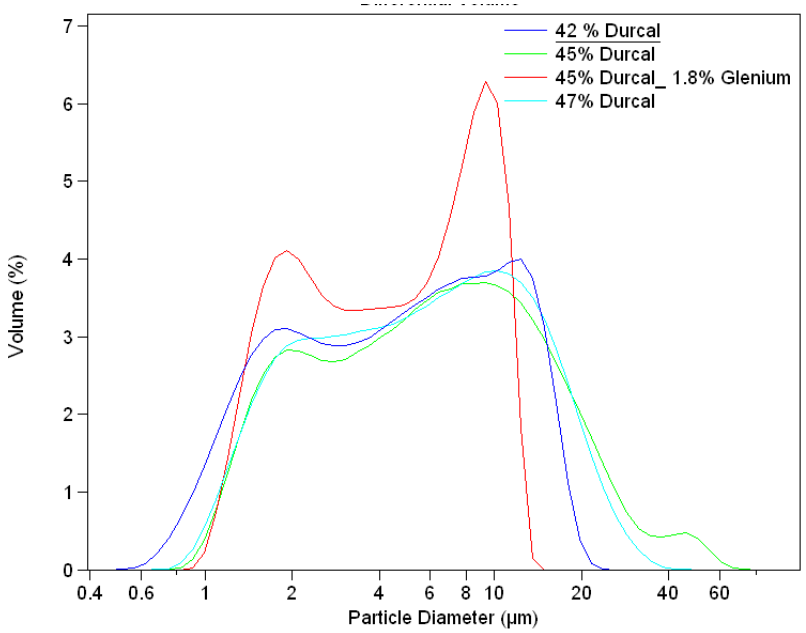

Figure 4.7: Suspensions with 47 vol.%, 45 vol.%, 42 vol.% and 45 vol.% Durcal 5 with 1.8 % Glenium after 24 h of preparation were measured by a laser particle size analyser at a pump speed of 9.

The further increase of maximum particle size at 45 % and 47 % volume fraction of Durcal 5 in between 40 μm and 65 μm must be a consequence of flocculation, due to the absence of such a particle size in the Durcal 5 powder.

The laser diffraction analyser could be capable to follow an evolution process of the flocs, however there could be some difficulties caused by dilution of the sample in water and the unknown impact of pumpspeed on floc structure.

4.5 FBRM® and PVM®

The FBRM® - ”Focused beam reflectance measurement” measures particle size distribution in-situ by a rotating laser beam. The light source is protected against the suspension by a saphire window with a diameter of 14 mm, which limits the maximum measureable particle size. The laser passes particles with a certain rotation speed and detects time of laser reflection. Due to the known rotation speed and time of laser reflection, particle size can be calculated. To decrease the random error, thousands of ”cord lengths” are measured.

The FBRM® software can analyse the data in macro or micro mode. In macro mode, the horizontal dashed line, which indicates the sensibility of analysis, is moved in bottom direction (see figure 4.8 b)). Therefore not only the peaks, where each peak

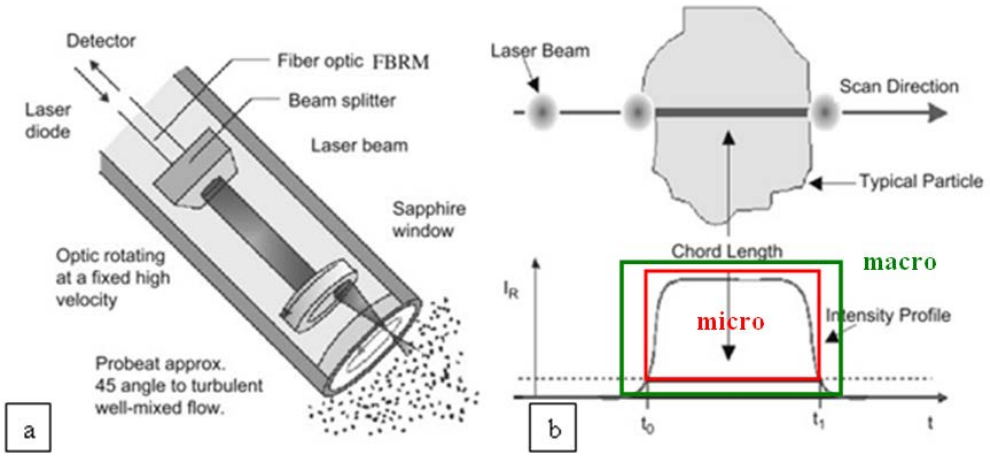

Figure 4.8: a) FBRM® setup. b) FBRM® chord length measurement with differents in micro and macro mode data analysis [10].

counts for the reflection of one particle, maybe fixed at a floc surface, but also floc connections deeper in the suspension and therefore resulting in a less intense signal, can be recorded. In very dense suspensions, the curve measured below the dashed line does rarely reach the bottom line caused by the low distance between particles and the continual reflection signal. At micro mode, the dashed line is moved in upper direction and therefore only peaks are measured. This reduces particle size at analysis for heterogenous floc surfaces due to the increase of sensitivity. Each chord length of a unique particle on the floc surface accounts for one peak as a result.

The PVM®- "Particle Vision and Measurement" is a visual in-situ observation device based on a CCD-camera chip enlightend by a white light source. It works like a digital camera where one pixel on the picture accounts for around 1 μm, therefore observation resolution is limited to around 5 μm.

4.5.1 Test execution

For test execution, a FBRM® G400 14 mm probe and a PVM® V819 probe from Mettler-Toledo were used.

Figure 4.9 shows the experimental setup of the PVM® and FBRM® measurement. The following suspensions were tested:

1. 42 vol.% of Durcal 5, idle time 3 days
2. 47 vol.% of Durcal 5 at fresh state
3. 47 vol.% of Durcal 5, idle time 3 days
4. 47 vol.% of Durcal 5, idle time 3 days with 1.8 % of Glenium

The sample was stirred at low speed and PVM® and FBRM® measurement were executed at the same time.

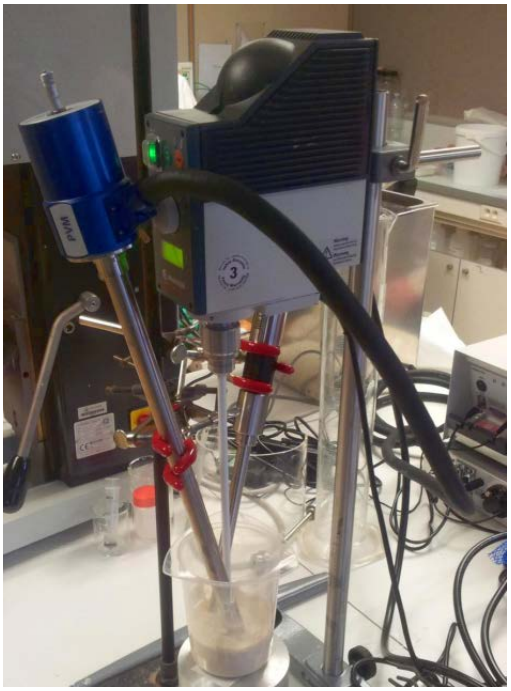

Figure 4.9: FBRM® from Mettler-Toledo at a suspension of 47 vol.% Durcal 5 and the glucose-water mixture.

The stirring speed of the Heidolph external mixer was increased stepwise from 25 rpm, 150 rpm, 350 rpm to 600 rpm. To reduce the random error, each speedstep was measured for 5 minutes. The evolution of the particle size distribution was measured by the FBRM®. The PVM® visualized the interior of the suspension with big black areas determined as air bubbles and white areas with a weak contrast as the partly flocculated calcium carbonate.

4.5.2 Results

The FBRM® measures ”cord lengths” which are statistically analysed and combined in a particle size distribution. The ”cord length” is very sensitive to particle shape due to its dependents on the passing way of the laser on the particle surface.

A suspension with 47 vol.% Durcal 5 and the glucose-water mixture, with an idle time of 3 days was measured. Various mixing speeds from 25 rpm to 600 rpm are applied during measurement. The horizontal axis shows the lengthscale for the mean particle size and the amount of particles in the different particle size fractions measured.

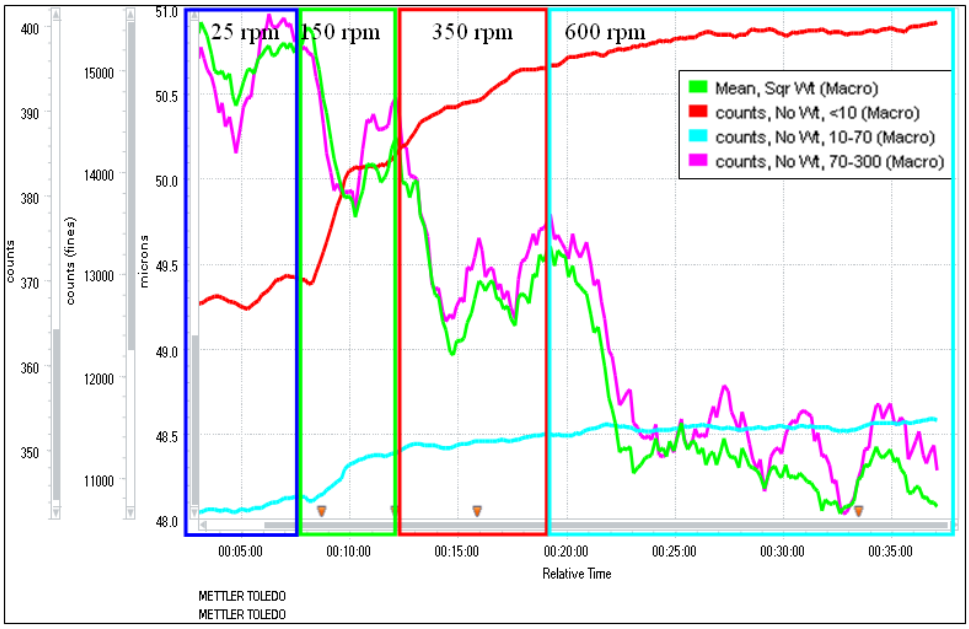

Figure 4.10: FBRM® results: Suspension of 47 vol.% Durcal 5 and the glucose-water mixture; idle time 3 days; mixing speeds from 25 rpm to 600 rpm during measurement; horizontal axis: lengthscale for the mean particle size and the amount of particles in the different particle size fractions

In general it can be stated, that with increasing rotation velocity, the particle size range from 70 μm - 300 μm and the mean particle size measured at macro mode decreases. At the same time, the amount of particles with a particle size inferior 70 μm and 10 μm considerably increases. This can be directly attributed to the deflocculation process caused by the impact of mixing. The mixing of the sample during measurement is necessary to increase the number of particles passing the laser light which decrease the random error.

Figure 4.11 summarises the results of the samples (enumeration in 4.5.1) 2, 3 and 4 (Sample 1 was measured only at two different stirrer speeds, 66 rpm and 100 rpm). The square-weighted mean chord length (a function of the average floc size) is plotted as a function of the stirrer speed.

Sample 2 (aged 47 vol.% without dispersant) shows a gradual and steady decrease in average floc size as the stirrer speed increases. Sample 3 (aged 47 vol.% with dispersant) shows a large decrease in average floc size as the stirrer speed is first increased from 25 rpm to 150 rpm, but thereafter the floc size stays approximately constant.

Sample 4 (fresh 47 vol.% without dispersant) shows a similar pattern to Sample 3, but the magnitude of the initial size reduction is much less [11].

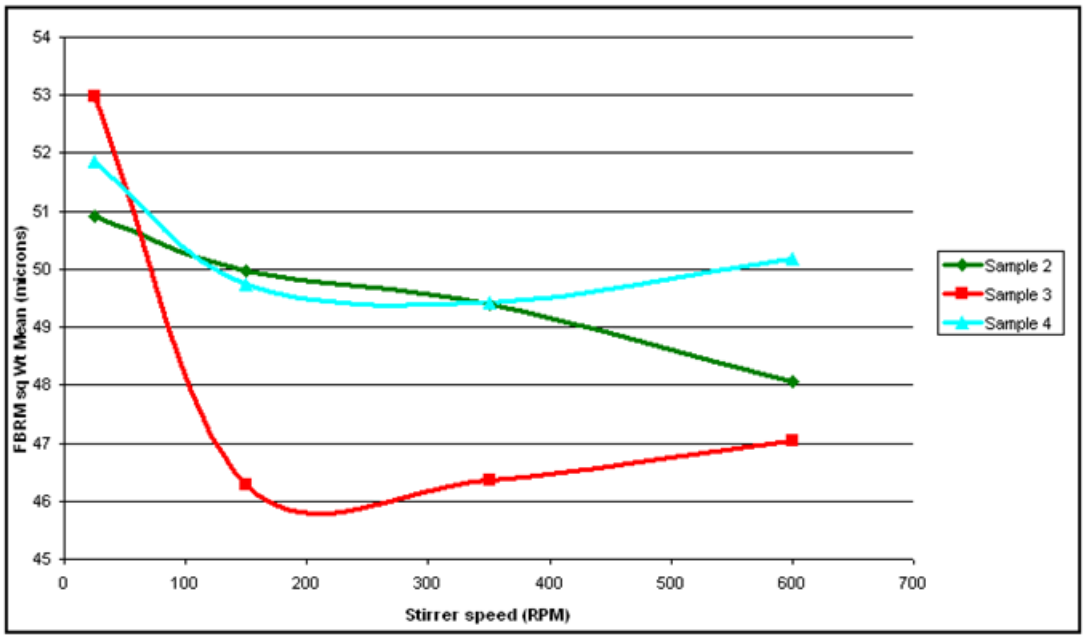

Figure 4.11: Evolution of particle size at increasing mixing speed measured by FBRM® for sample 2 (47 vol.% Durcal 5, 3 days aged), sample 3 (47 vol.% Durcal 5 plus 1.8% Glenium, 3 days aged) and sample 4 (47% Durcal 5 at fresh state) [11].

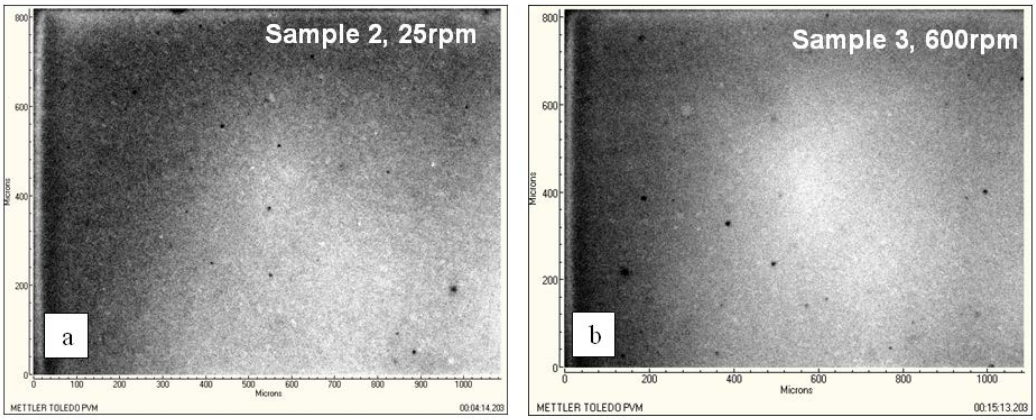

Figure 4.12: PVM® picture for the aged sample at 47 vol.% Durcal 5 with mixing at a) 25 rpm and b) 600 rpm [11].

The figure shows black points which are stable air bubbles in the sample due to the yield stress present. Durcal 5 can be seen as white fraction in the suspension.

4.5.3 Conclusion

The FBRM® has the ability of in-situ measurements in dense opaque suspensions with a minimum particle size of 500 nm.

The change from macro to micro mode strongly influences the obtained results. The micro mode is not capable to measure floc size in total and gives only results about unique particle size. At macro mode, total floc size can be measured. Caused by the reduction in sensitivity, it is difficult to distinguish between small gaps and weak floc bondings. In that manner the results don't match real particle size distribution.

The resolution of the PVM® as an additional measurement device is not high enough and therefore doesn't obtain usable data concerning modelling of flocculation.

A suspension of 47 vol.% of Durcal 5 is too dense for the FBRM® measurement, caused by the low distance in between particles and failure induced by macro mode measurement. To solve this problem, the suspension should be diluted in water or in the glucose-water mixture. The bigger distance in between particles would help to improve the accuracy of measurement at macro mode.

4.6 X-ray microtomography

The X-ray microtomography measurement is based on the principle of X-ray absorption, diffraction and transmission. The X-ray wavelength is in between 10 nm to 0.01 nm. It penetrates easily matter with small density and is absorbed by dense materials. The minimum voxel size is 5 μm with the radiation source used at Laboratoire Navier. The radiation source is a closed tube source with 130 kV. Due to the 3D scan, voxel is used instead a pixel, which corresponds to a cube with a certain side length. The contrast in the picture depends on density and the position of the elements in the periodic table.

The X-ray source produces X-ray radiation by the acceleration of electrons by high voltage and the collision on a metal target. Two sources of X-ray exist. The first source is a X-ray tube with a polychromatic-conic beam and a low brilliance. It is used at all labortatory X-ray microtomography devices without a Synchrotron radiation source. As a second radiation source, a Synchrotron, which can produce an almost monochromatic, parallel beam with a high brilliance, is used. This helps to increase resolution and to decrease scanning time.

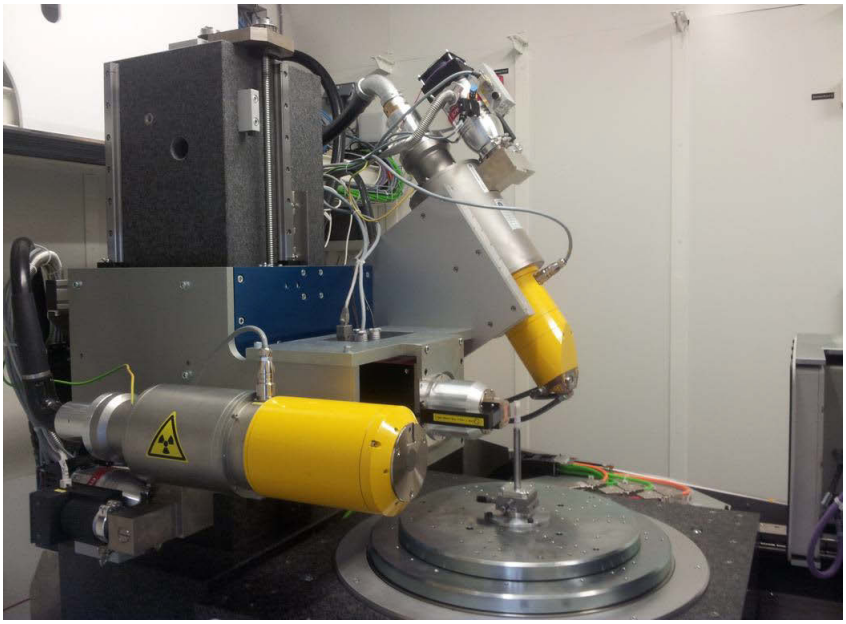

Figure 4.13: X-ray microtomography at Ecole des Ponts ParisTech.

4.6.1 Test execution

The suspension was inserted in a plastic tube by a pipette with a diameter of 8 mm. A plastic tube was used to reduce the disturbance of the signal. The sample was prepared 3 days in advance to observe the sample in a flocculated state and to eliminate further evolution during the measurement time of 3 hours. For the testing, a suspension of 47 vol.% Durcal 5 with a glucose-water mixture stirred by a Heidolph blender for 1 minute at 500 rpm, was used.

4.6.2 Results

In figure 4.14, the results of the X-ray microtomography measurement can be observed.

The resolution of 6 μm minimum voxel side length is not high enough to gain information about flocculation and final structure in the suspension. The image demonstrates, that the content of air bubbles is high in the suspension. It is only possible to observe a grey suspension but grain boundaries are not visible.

4.6.3 Conclusion

A radiation source with a higher resolution will be installed in April 2013. The new radiation source will have a potential of 160 kV and works with a resolution of

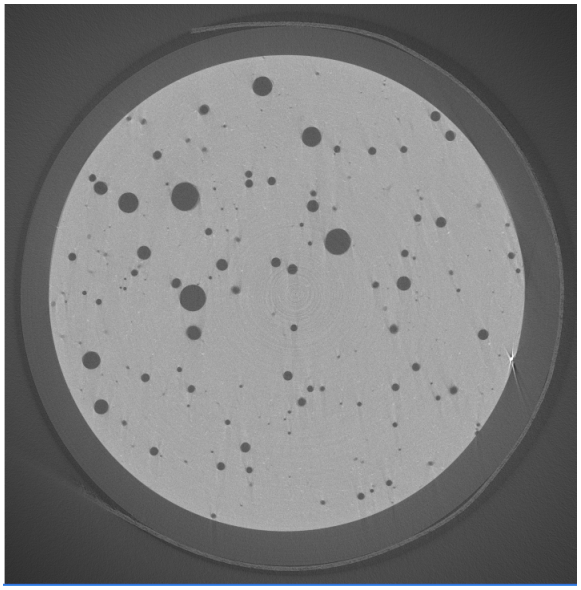

Figure 4.14: A suspension of 47 vol.% of Durcal 5 with glucose-water mixture was tested after 3 days of idle time. The dark grey circles show stable air bubbles.

0.25 μm voxel side length. The aquisition time of a tube X-ray microtomography is too long to follow an evolution process in the suspension, it can thus only help to understand a final state of flocculation. The new radiation source can gain potentially very interesting information. A Synchrotron light source does reduce the aquisition time from 3 hours to a few seconds, which enables to follow an evolution process, with the disadvantage of difficult accessibility to the Synchrotron.

4.7 Rheometry

The rheometer tests were performed with a Bohlin C-VOR high resolution rheometer. The requirement for the sample was a measureable evolution of yield stress and stable testing conditons for at least 24 hours.

4.7.1 Rheometer and geometry applied

The Bohlin C-VOR is a high resolution rheometer which is capable to measure at controlled stress, strain or shear rate. The measurement geometry consists of a rotating bob (inner cylinder), located in a fixed cup (outer cylinder). The inner cylinder has a diameter of 2.3 cm and the outer cylinder 3.6 cm. The rotation of the inner cylinder causes the movement of the suspension in the annular gap.

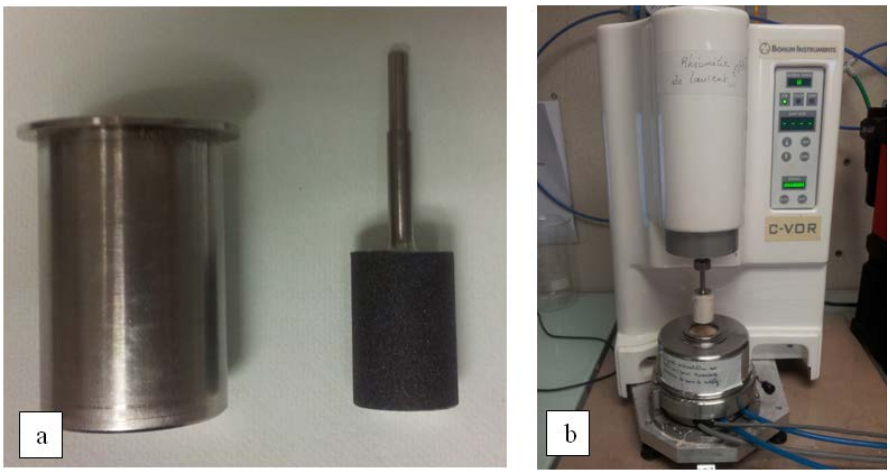

Figure 4.15: a) Coaxial cup and rotating bob geometry used at the rheometer, inner cylinder 2.3 cm, outer cylinder 3.6 cm, 180-grid sandpaper fixed on the surface. b) Bohlin C-VOR high resolution rheometer used for rheometer measurement.

To avoid effects of sliding on the cylinder surface, 180-grid sandpaper is fixed on the surface to improve friction.

Advantages of coaxial cup and bob geometry are the efficient temperature control, the good repeatability and the use of suspensions with bigger particles. As a disadvantage can be pointed out the slight variation of stress over the gap.

The temperature controlling system is vitally important due to the strong dependency of viscosity on temperature. In the laboratory a Julabo FP50 - Cryostar is used to cool the sample.

4.7.2 Test execution

The testing started at 43 vol.% of Durcal 5 and was increased doing tests with 47 vol.% to improve the effect of flocculation.

The sample was mixed by an external Heidolph RZR2102 control blender with 500 rpm for 1 minute. The low speed was important to avoid an increase of suspension temperature. The external mixing was performed at 22 °C ambient temperature. After external mixing, the suspension was filled in the temperature controlled cup (outer cylinder) of the rheometer. The Cryostar fixed temperature at 20 °C.

To gain knowledge about the rheology of the model material, it was necessary to find stable testing conditions. This was reached by a idle time (time without mechanical impact) of 24 hours. After 24 hours, the sample was mixed in the rheometer at 180 Pa for 300 seconds. The idle time was increased at each testing. According to Barnes

[2], the impact on flocculation by mixing is a few orders of magnitude higher than just by brownian motion, therefore the initial state of flocculation after external mixing had to be studied more in detail.

Following, the testing was concerned on repeatability of the testing and the reachability of an initial state. A test sequence was carried out at constant stress and increasing stirring time, to gain knowledge about the mixing time necessary to reach an initial deflocculated state.

Subsequently, the test procedure was a combination of repeated strong mixing, a certain idle time and a measurement period. The repeated mixing was performed at a shear stress of 2000 Pa for 1500 seconds. This was necessary to break down flocs or structure and to obtain a ”compareable” intial state and repeatable testing conditions at fresh state. The term compareable initial state is related to the problem, that a great uncertainty remains about the initial state of flocculation directly after mixing.

After a specific idle time, the shear stress was measured for a period of 1000 seconds at constant 0.01 rpm deformation. The measured yield stress was read out after a measurement time of 800 seconds. To improve accuracy of the testing results, the measurement procedure was repeated 5 times and an average value was used. The idle time was increased from 0 seconds to 600, 1200, 2400, 3600, 7200, 10800 and 36000 seconds and the increase of yield stress was registered.

4.7.3 Results

At the beginning, an initial idle time of 24 hours was choosen due to the repeatablility of measurements obtaining constant values of yield stress at small idle time.

In Figure 4.16, the evolution of yield stress in a suspension with 43 vol.% Durcal 5 with applying different idle times, can be seen. After preparation and an idle time of 24 hours, the sample was mixed before each measurement sequence for 300 seconds at a stress of 180 Pa, to break down flocs. Before stress measurement, a different idle time was applied. The test was repeated with the same sample, idle time was increased from 0 to 5 hours with the denoted mixing circle after each measurement. The results presented in figure 4.16 showed the yield stress evolution with time. The increasing time shown in the legend denote for certain idle times applied during testing. The curve without a peak at 0 seconds idle time shows, according to Pignon [22], a structure formation process with the increase of yield stress until a constant level. At an idle time of 300 seconds, the red curve illustrates already a breakdown of structure with a peak at the beginning and a decrease until a certain level. At an

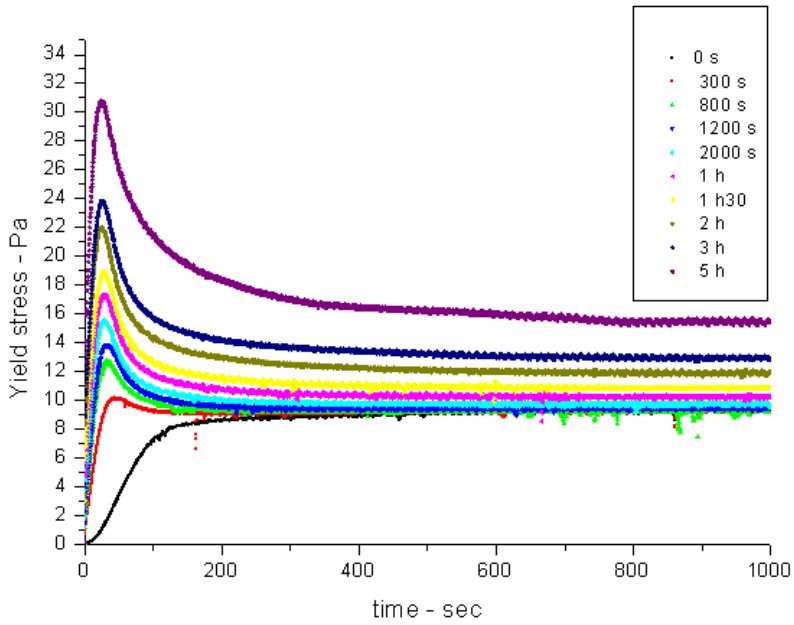

Figure 4.16: Yield stress formation with applying different idle times.

idle time of more than 1.5 hours, a significant increase of yield stress with time is visible.

According to Barnes [2], the colloidal forces holding the structure together, are acting over a short distance of about 10 nm. Therefore, the impact of flocculation was increased by the raise of volume fraction from 43 vol.% to 47 vol.% of Durcal 5. Barnes further points out, that at idle time, only brownian forces are present, which are a few orders of magnitude smaller than the shear force introduced by mixing. Thus the rebuilding of structure or flucculation with the rearrangement of particles to flocs and further to complex structures takes a long time and is accompanied by the increase of viscosity and yield stress.

Due to the very strong impact of shear stress by initial mixing compared to brownian motion at idle time, it was further important to study the flocculation state present directly after initial mixing.

Different sequences of increasing mixing time at a stress of 2000 Pa were executed on a fresh sample. The yield stress measurement was started after 600 seconds of idle time to avoid an influence of temperature increase by mixing on viscosity and yield stress.

Figure 4.17 shows repeatability testing at different mixing time. The mixing and measurement circle is repeated 5 times with the same mixing time and the same sample. This repeatability testing is executed for the indicated mixing times of: 300 s, 1500 s, 2000 s and 3000 s. Each Sample is newly prepared when mixing time is

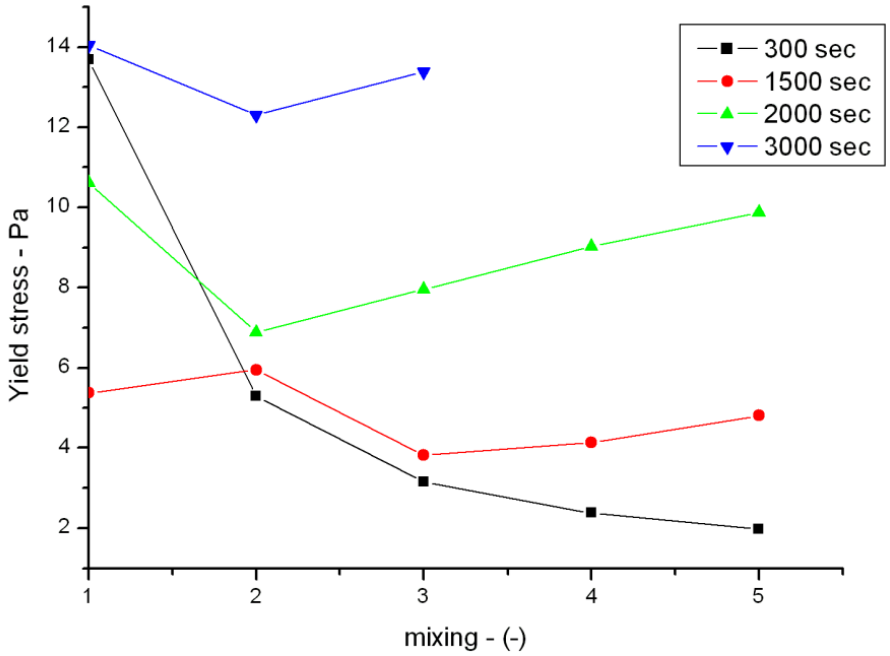

Figure 4.17: Repeatability mixing testing: Stress formation at different mixing times.

changed. The results in figure 4.19 demonstrate the difficulty to obtain an initial deflocculated state by mixing. At a mixing time of 300 seconds, the initial yield stress is high and decreases continually with further mixing. This exemplifies, that the mixing time is not long enough due to further decrease of yield stress, which can be assumed as a further breakdown of structure. The low values after 5 times of 300 seconds mixing can be either explained by the breakdown of structure and the further improvement of alignment of flocs into shear direction, causing lower yield stress or a continuous breakdown of flocs.

At a mixing time of 1500 seconds, the values obtained scattered around 5 Pa yield stress. This illustrates, that almost the same initial state could be reached due to a compareable yield stress evolution after identical idle time at repeated tests. A problem is the interpretation of the higher values of yield stress at 1500 seconds of mixing compared with the 2^{nd} until the 5^{th} measurement at 300 seconds of mixing time. Logically, a longer mixing time should lead to a further break down of flocs and structure and should therefore result in lower yield stress, which is not the case. It could be concluded, that either the impact on suspension causing a breakdown of flocs was still not strong enough at 1500 seconds of mixing time, measuring therefore just the rebuilding of structure in the suspension or the impact was strong enough to break down flocs but initial flocculation and the rebuilding of structure proceeds faster at a more deflocculated state.

The increase of mixing time up to 2000 seconds and 3000 seconds leads to a further increase of yield stress. In this context has to be mentioned, that the temperature in the sample can considerably increase at very long mixing times also in combination with a temperature controlling system. This could lead to a decrease in viscosity and a strong flocculation due to increased brownian motion and the impact of shear force immediatly after mixing.

Within the scope of the Master's thesis, it was not possible to investigate the state of flocculation directly after mixing more in detail, this should be done by further testing within the subsequent PhD thesis.

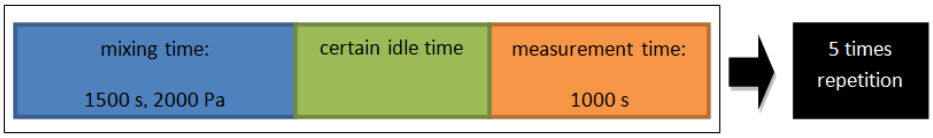

Figure 4.18: Yield stress evolution testing sequence. At each of the 5 repetitions, idle time and the sample is the same and an average of the five results obtained, is calculated. The average values at certain idle time can be seen in figure 4.20 a).

A mixing time of 1500 seconds at 2000 Pa was chosen for further testing, assuming a low degree of flocculation or structure present in the sample and a high compliance of repeated tests.

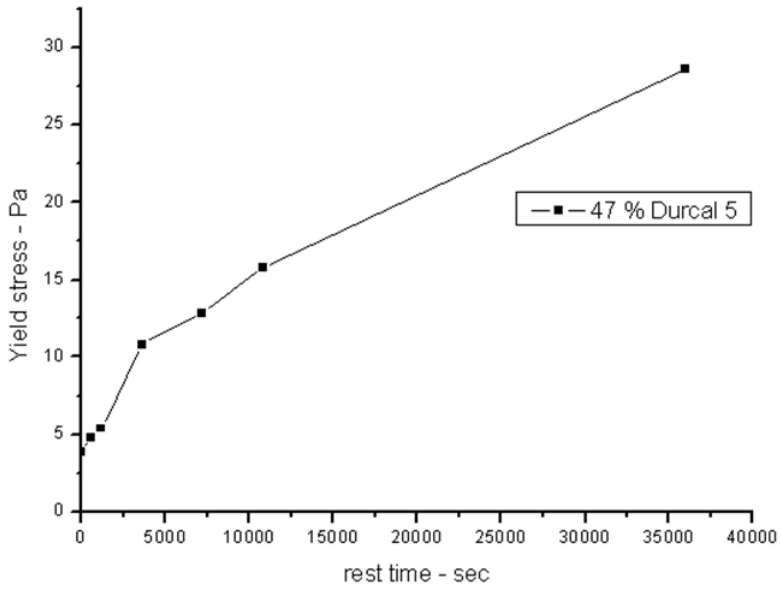

Figure 4.19: Yield stress evolution with time at 47 vol.% Durcal 5 after 800 s of yield stress measurement. Coaxial cup and bob geometry; inner cylinder 2.3 cm, outer cylinder 3.6 cm; 180-grid sandpaper fixed on the surface

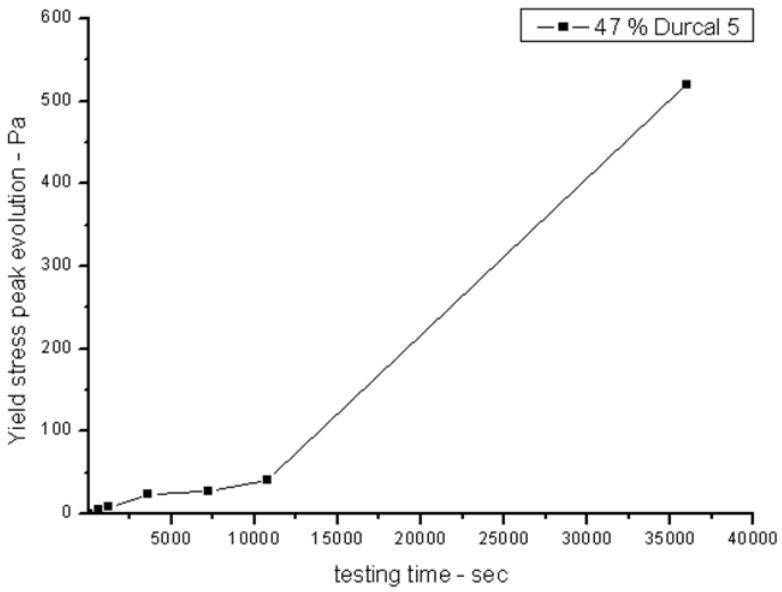

Figure 4.20: Increase of initial peak hights at the yield stress measurement. Coaxial cup and bob geometry; inner cylinder 2.3 cm, outer cylinder 3.6 cm; 180-grid sandpaper fixed on the surface

The yield stress evolution was measured at 47 vol.% Durcal 5. At each idle time indicated by a point in figure 4.20 a), a sequence consisted of 5 repetitions of 1500 seconds mixing time at a stress of 2000 Pa, certain idle time and a measurement time of 1000 seconds, was executed. The yield stress was read out at 800 seconds of measurement time and an average of all 5 measurements was taken. After each change of idle time measurement, the sample was freshly prepared.

Figure 4.19 shows a strong increase of yield stress within the first 3600 seconds from 4 Pa to 11 Pa, a decrease of yield stress evolution until the 3^{rd} hour and a further flattening of the curve until the 10^{th} hour. The evolution of yield stress can be related to the increase of floc size due to the break down of structure by the small deformation introduced by the rheometer until 800 seconds of measurement.

In Figure 4.20, the evolution of the initial peak can therefore be directly related to the break down of structure by small deformations at the beginning of the measurement. Between 3 hours and 10 hours of testing, the peak strongly increases, which could be a hint, that structure formation takes place mainly after 3 hours of idle time.

The X-ray microtomography measurement revealed furthermore a presence of a big volume fraction of stable air bubbles in the suspension. According to Kogan [20], air bubbles have no influence on evolution or change in yield stress.

4.7.4 Conclusion

The rheometer is a very exact and powerful measurement tool to follow an evolution process in a suspension by measuring change in viscosity, yield stress, storage modulus *G'* and loss modulus *G"*. It has the further advantage of temperatur controllability.

At subsequent testing, big and homogenised amounts of the glucose-water mixture have to be prepared in advance to avoid influence of systematical change of viscosity by change of glucose source. Furthermore, the initial sample preparation and mixing time has to be examined more in detail to obtain information about the state of flocculation at initial state after mixing.

The evolution of yield stress and the initial peak at the yield stress measurement could help to distinguish between flocculation and structure formation in the sample.

During the subsequent PhD thesis, an extension of yield stress evolution for a wider range of volume fractions should be studied, to obtain a broader base of data for flocculation modelling.

4.8 Minispec

The Bruker Minispec mq20 is a 20 MHz NMR spectrometer with a magnetic field of 0.5 T. It is used to measure longitudional and transverse relaxation time of ^{1}H. The sample diameter is 10 mm with a sample volume in between 1 ml and 2 ml.

4.8.0.1 Test execution

At the beginning, the relaxation time of T1 and T2 were determined, which showed a higher sensitivity of transverse relaxation time T2 at different volume concentrations of Durcal 5. Afterwards, a procedure was executed to determine the linear relation for different concentrations of Durcal 5 and the relaxation time T2 necessary to receive the incline which is denoted as ε and necessary for further calculations used in formula 4.11.

Afterwards, concencrations of 30 vol.%, 40 vol.% and 47 vol.% volume fraction of Durcal 5 mixed with the glucose-water mixture and for comparison also with certain amounts of Glenium, were used. The sample was mixed by a Heidolph RZR2102 control blender with 500 rpm at ambient temperatur of 22°C. Between 1 ml and 2 ml of the suspension was inserted in a test tube and the test tube was inserted in

the Minispec. The sample temperature in the Minispec was regulated at 20°C by a Huber Ministat temperature controlling system.

The evolution of the relaxation time T2 was measured for 15 hours. The goal of the relaxation time measurement was to relate relaxation time with the change in concentration by:

$$\frac{1}{T_2} = \frac{1}{T_0} + \varepsilon \frac{c}{1-c} \tag{4.1}$$

The transverse relaxation time T2 is measured by the Minispec. The relaxation time T0 is the relaxation time of the glucose-water mixture without solids. The constant ε is calculated in advance by the rearrangement of the formula and the measurement at different concentrations of Durcal 5. The concentration c is the volume fraction of Durcal 5.

The diffusion coefficient of ^{1}H in the glucose-water mixture was measured by the use of the magnetic gradient at the Minispec. The diffusion coefficient is 2.3 * 10^{-10} $m^2 * s^{-1}$ which results in a diffusion length of around 4 μm of the ^{1}H nuclei. The diffusion length is the sensitive length scale for Minispec measurements in the suspension.

4.8.0.2 Results

Regions with high concentrations of particles like flocs show short relaxation time and regions with low concentration of particles, show long relaxation times.

The graph 4.20 illustrates the analysed data obtained by the Minispec. A biexponential fit is required to analyse the data. The mean value and the derivation of the longest time component throughout the sample were combined to calculate average concentration and positive and negative scattering. The average concentration does change slightly during measurement, which can't be explained for the moment. The positive and negative deviation show regions with high and low concentration of particles and the evolution with time. It can be derived, that regions with high concentration tend to increase in concentration and regions with low concentration tend to show a revers behavior.

This can explain flocculation by coagulation of particles on already existing agglomerations, leaving less concentrated regions.

Figure 4.21 shows the evolution of change in concentration with time for suspensions with 30 vol.%, 40 vol.%, 47 vol.% and 47 vol.% Durcal 5 with 1.8 % of Glenium. The change in concentration can be either caused by flocculation of particles or

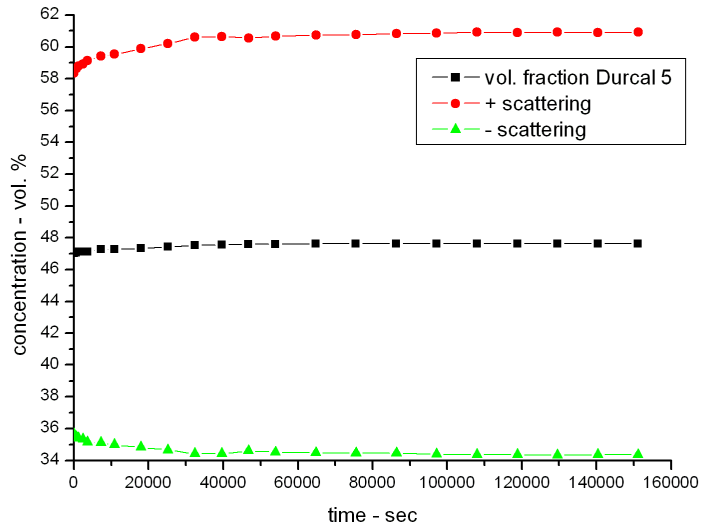

Figure 4.21: Results of local change in concentration with time measured by the Bruker Minispec at a suspension of 47% of Durcal 5 and the glucose-water mixture.

sedimentation. By the use of the glucose-water mixture, sedimentation doesn't take place at high volume fractions and within 24 hours of measurement. This was proved by the concentration profile measurement at the MRI and the Turbiscan testing.

The temperature as influencing factor can be excluted in this graph, because the second point is already measured at equilibrium temperature.

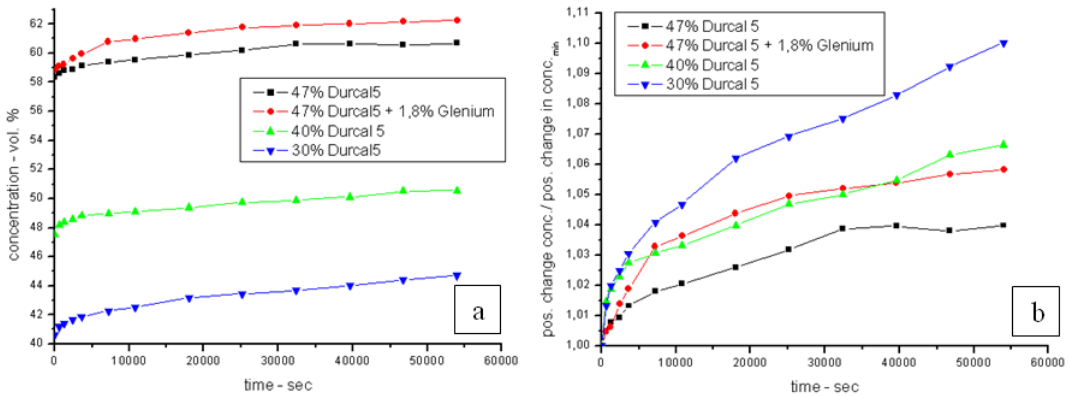

Figure 4.22: Results of local change in concentration with time measured by the Bruker Minispec for samples of 30 vol.%, 40 vol.%, 47 vol.% and 47 vol.% of Durcal 5 with 1.8 % of Glenium.

The high change in concentration at less concentrated suspensions can be denoted to the presents of more free space around particles, giving more space for motion. Hence it can't be explained as stronger impact of flocculation compared to the sample with 47 vol.% Durcal 5.

The bigger change in concentration for the sample with 1.8 % of Glenium compared to the sample without Glenium at 47 vol.% Durcal 5 can be explained by the stronger movement of particles due to repulsive forces caused by the dispersing agent observed already at the transmitted light microscope.

It has to be pointed out, that the change measured by the Minispec in average concentration of particles is still not understood and has to be studied further.

4.8.0.3 Conclusion

According to executed tests, it can be concluded, that the Minispec is capable to measure an evolution process from a homogenous to a more heterogenous state in a dense opaque suspension. The measurement shows a fast evolution within the first hours. The Minispec can give important information concerning time scale of reaction and intensity of structure formation.

4.8.1 Magnetic resonance imaging

The Imager: Bruker Biospec 24/80 DBX is a Magnetic resonance imaging (MRI) device. It is used to obtain information about complex materials and fluids [18]. The maximum sample diameter is 20 cm and limited by the surrounding radio antenna. The magnet consists of a superconducting magnetic coil which is cooled by liquid helium and liquid nitrogen.

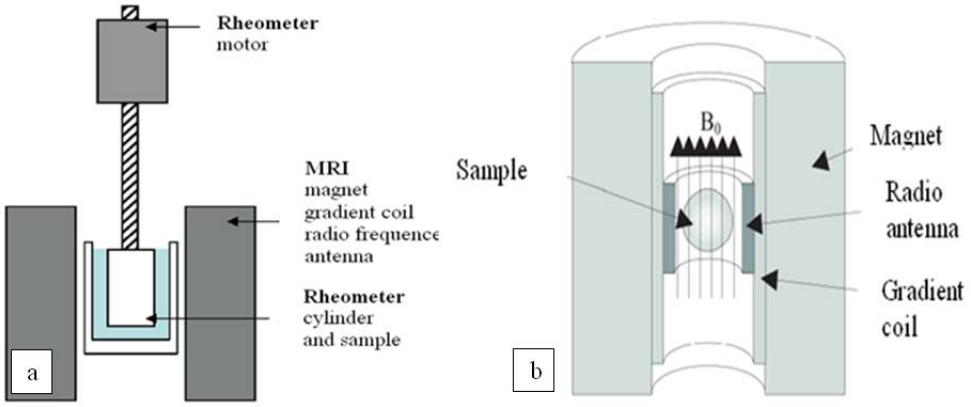

Figure 4.23: a) Setup of the MRI with the rheometer used. b) Explanation of components in the MRI device.

By the use of a magnetic field gradient, which employs a weaker magnetic field, nuclei rotate at different locations with different speed. Therefore the magnetic field is composed of:

$$B(\vec{r}) = \dot{B}_0 + \vec{G}\vec{r} \tag{4.2}$$

where $\vec{G}$ denotes the field gradient. Accordingly, the resulting frequence is:

$$\omega(\vec{r}) = \gamma B(\vec{r}) \tag{4.3}$$

$$\omega(r) = \omega(0) + \gamma\vec{G}\vec{r} \tag{4.4}$$

This gives the opportunity to localize spatially according to Hafid [9]. The temperatur is measured by a sensor and a fiber optic device which is fixed on the outer surface of the outer cylinder.

4.8.1.1 MRI-rheometer

The magnetic resonance imaging device is coupled with a rheometer. The rheometer consists of a motor mounted above the MRI device and a shaft where the inner rotating cylinder is fixed. The rotating velocity is in between 0.01 rpm to 400 rpm. The suspension is inserted in a statical cylinder with a diameter of 12 cm. The diameter of the inner rotating cylinder is 8 cm.

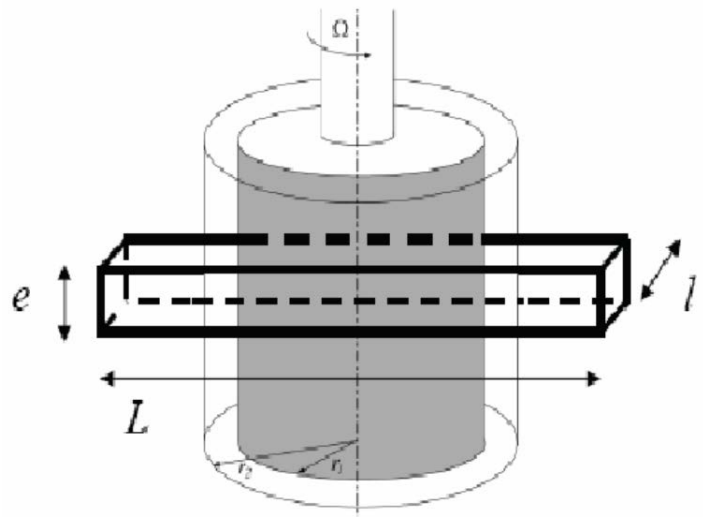

Figure 4.24: Geometry of the rheometer.

The surface is napped by a 180-grit-paper to improve friction in between the suspension and the rotating cylinder. The napping of the surface helps additionally to avoid the use of grit-paper fixed on the surface, which causes disturbances on the MRI image.

4.8.1.2 Concentration Profile

The concentration profile gives information about local concentration in x - y - z direction. The concentration profile shows change in concentration in comparison with an initial concentration profile. The localisation is possible due to the use of the magnetic field gradient.

The concentration profile helps to identify sedimentation or immigration of particles in radial direction caused by centrifugal force.

The analysis is based on the comparison of an initial state to an advanced state. Change in concentration is calculated by:

$$\delta c = \frac{I_1 - I_0}{I_0} \tag{4.5}$$

I_1 is the concentration profile of the aged sample and I_0 is the concentration profile of the sample in initial state.

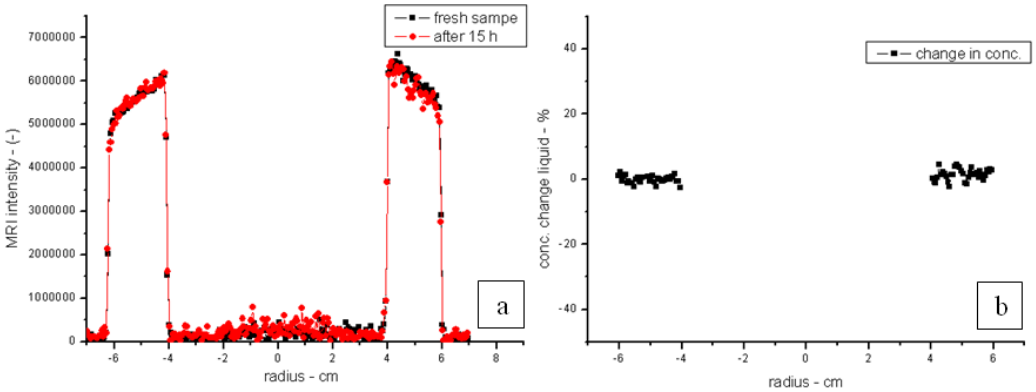

Figure 4.25: a) Concentration profile in radial direction of a suspension with 47 vol. % Durcal 5 and the glucose-water mixture before mixing and after the mixing process and 15 hours of idle time. b) Change of concentration in radial direction of the liquid in %.

Figure 4.24 shows the concentration profile in radial direction. It must be stated, that the MRI measurement is only sensitive to the liquide phase, therefore it shows the change in liquid concentration. The initial concentration profile was measured

before the initial mixing process in the MRI device. The second concentration profile was measured after mixing of several minutes at 300 rpm (see at test execution) and an idle time of 15 hours. In figure 4.24, no remarkable immigration of particles in radial direction can be seen. Thus centrifugal force didn't lead to a densification in the outer regions.

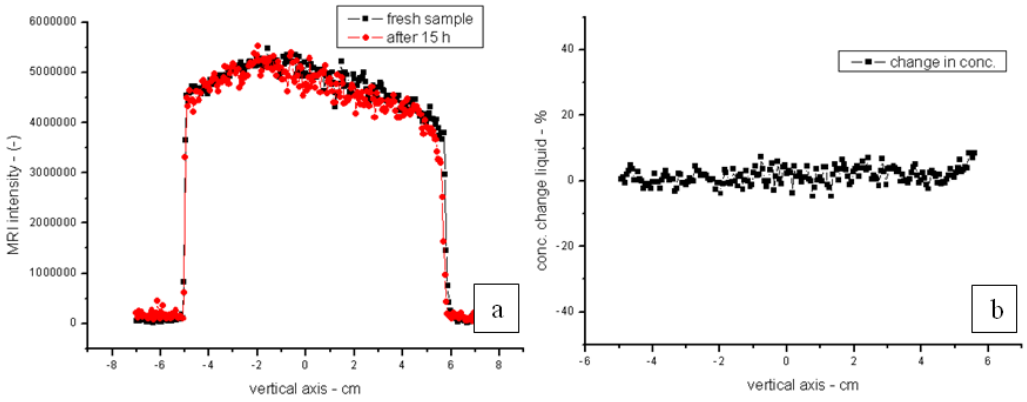

Figure 4.26: a) Concentration profile at the vertical axis of a suspension with 47 vol.% Durcal 5 and the glucose-water mixture before mixing and after the mixing process and 15 hours of idle time b) Change of concentration of the liquid in %.

In the concentration profile in vertical direction, no serious change in concentration can be observed with time. A small deviation occurs at the top of the sample which could be attributed to a process of drying at the surface. The concentration profile in vertical direction is an evidence for the stability of the sample concerning sedimentation.

4.8.1.3 Velocity profile

In the velocity profile, the velocity distribution of the suspension in the annular gap between the inner and the external cylinder can be seen.

At velocities above 10 rpm, the velocity profile is almost linear at the fresh sample a) and the sample b) with an idle time of 15 hours (see figure 4.27). At lower speed, the region of the annular gap where no movement is present increases at the fresh sample at 1 rpm to a radius of 0.054 cm and for 0.5 rpm to a value of 0.05 cm. The sample with an idle time of 15 hours shows already an evolution at 3 rpm to a radius 0.054 cm and a further increase to 0.05 cm and 0.049 cm for 1 rpm and 0.5 rpm.

The region without movement increases due to the increase in yield stress in the sample. Further explanations can be found at the flow curve calculation.

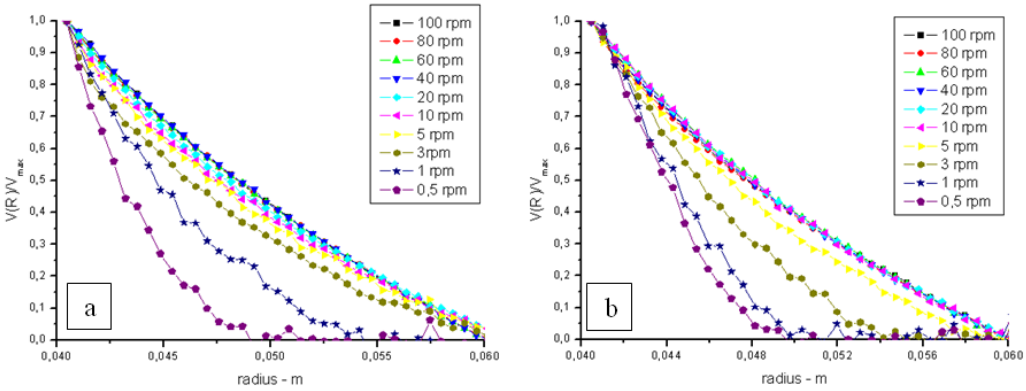

Figure 4.27: Velocity profile of a suspension with 47 vol. % Durcal 5 and the glucose-water mixture. a) Velocity profile at fresh state of the sample. b) Velocity profile after 15 hours of idle time.

With the results of the velocity profile and the resulting torque measured by the rheometer, the flow curve can be calculated.

The flow curve shows the shear rate on the x-axis dependent on a certain stress on the y-axis.

The stress $\sigma_{r,0}$ is calculated by the torque Γ measured at the rheometer for the geometry used, devided by $2\Pi r^2 H$ where H denotes the height of the inner cylinder, submerged in suspension.

$$\sigma_{r,\theta} = \frac{\Gamma}{2\Pi r^2 H} \tag{4.6}$$

The shear rate is, according to Ovarlez [21], the derived from the local velocity profil in cylindrical coordinates.

$$\dot{\gamma} = -r \frac{\partial}{\partial r} \frac{v}{r} \tag{4.7}$$

Concluding, the flow curve is build up by the torque at certain velocities and the resulting yield stress.

4.8.1.4 Test execution

For the MRI testing, a suspension of 47 vol.% of Durcal 5 and the glucose-water mixture was used. For each testing, 1200 g of suspension was prepared to fill the annular gap in between the inner and the outer cylinder. The suspension was roughly mixed with an external plastic blender before the insertion into the MRI. The rheometer

in the MRI was used to mix the suspension at a velocity of 200 rpm - 300 rpm to obtain a homogenous suspension and to reach an initial state. During the first mixing process at a volume fraction of 47 vol.%, the suspension was warmed up within 7 minutes from 20 °C to 28 °C due to the non existing temperatur controlling system and the very high viscosity. To avoid the impact of temperature increase with a strong influence on viscosity, the calcium carbonate was stored for 12 hours in a freezer at -12 °C and the glucose-water mixture in a refrigerator at 2 °C. The suspension was also roughly mixed by an external Heidolph mixer and stirred by the MRI rheometer at a speed of 300 rpm for 6 to 7 minutes until it reached the temperatur of the radio antenna, which was 20 °C.

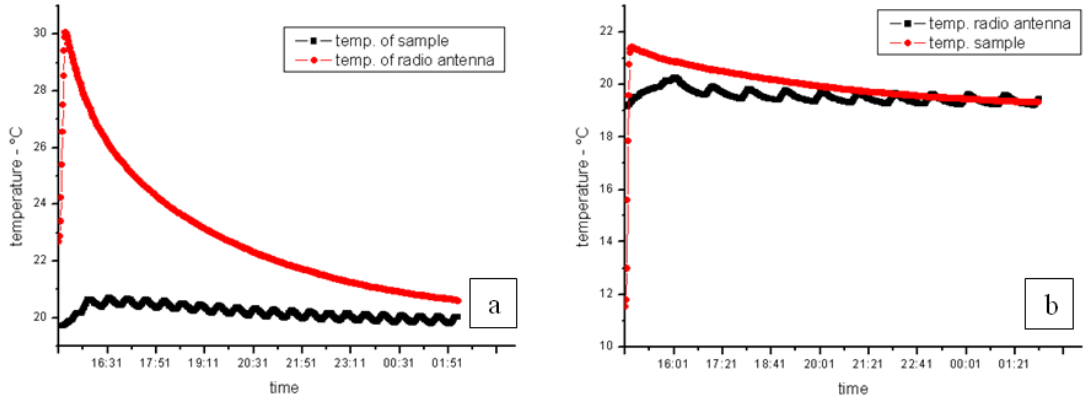

Figure 4.28: Initial mixing in the MRI-rheometer of a suspension with 47 vol.% Durcal 5 at: a) Without cooling, the sample was stirred 2 minutes at 200 rpm and 5 minutes at 300 rpm. b) With cooling, Durcal 5 in the freezer and glucose-water in the fridge. Mixing of 2 minutes at 200 rpm and 5 minutes at 300 rpm.

After mixing, a concentration profile in x, y and z direction and a velocity profile at 0.5, 1, 3, 5, 10, 20, 40, 60, 80 and 100 rpm was carried out. Following, different sequences where started.

	rotations (rpm)	**time** (h)
28 °C sample	0,5	15
20 °C sample	0,5	15
20 °C sample	1	66
20 °C sample	0	15

Table 4.1: Test sequence at 28°C and 20°C with different idle time.

After the execution of a testrun, a second velocity profile with increasing velocities was carried out.

4.8.1.5 Torque measurement

The torque was measured at the laboratory rheometer with the same geometry like at the MRI device.

For the torque measurement, the value C1 and C2 of a coaxial cylinder had to be calculated to define the geometry of the sample at the rheometer. Further it was important to change the height of the cylinder at C1, if the immersion depth was decreased to 4cm and 2cm.

$$C1 = \frac{1}{2\Pi {r_a}^2 H} \tag{4.8}$$

$$C2 = \frac{2{r_i}^2{r_0}^2}{{r_a}^2({r_0}^2 - {r_i}^2)} \tag{4.9}$$

Due to the high viscosity of the suspension, only small values of torque could be measured at the same immersion depth of the cylinder present at the MRI. The total immersion deepth at the MRI was 8.3 cm. For the torque measurement, higher velocities were executed at an immersion depth of 4 cm and 2 cm and the results were shifted to fit with the small velocities measured at maximum immersion depth. Due to the raise of the inner cylinder, to reduce immersion depth, the remaining suspension below the inner cylinder was not homogeneously mixed, which could show an impact on the final torque curve. For this reason, torque measurement must be executed in future by the decrease of suspension volume until a maximum immersion depth of 8.3 cm of the inner cylinder, instead of lifting the inner cylinder. This is important, to mix the whole sample volume homogeneously.

According to Ovarlez [21], linear torque evolution can be assumed to be valid at higher velocities. Due to the initial break up of structure and the further deflocculation, the torque curve could show a small deviation from linear behavior. It remains still a great uncertainty about the correct measurement of tourque at high viscosity which has to be investigated more in detail within the subsequent PhD thesis.

4.8.1.6 Results

Figure 4.30 demonstrates the flow curve of a suspension of 47 vol.% Durcal 5 mixed with the glucose-water mixture after 15 hours of idle time. Due to the uncertainty of torque measurement, the results still have to be treated with caution.

A linear Newtonian fluid is outlined by the inserted line. At a speed range from 5 rpm to 20 rpm, the behavior is almost Newtonian (linear). At higher rotation speed,

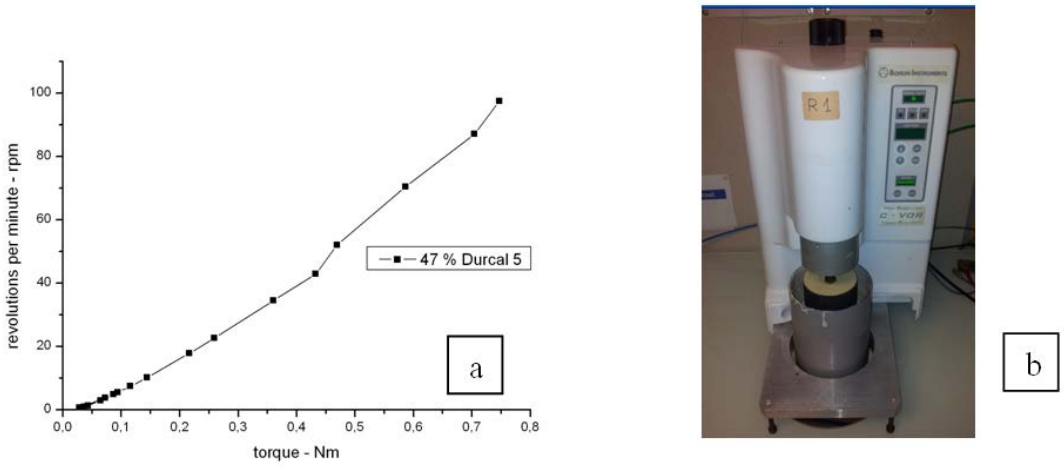

Figure 4.29: Torque measurement executed at Bohlin C-VOR rheometer with the MRI geometry showed in figure 4.29 (inner diameter: 12 cm and external diameter of 8 cm). The torque was measured at a sample with 15 hours of idle time.

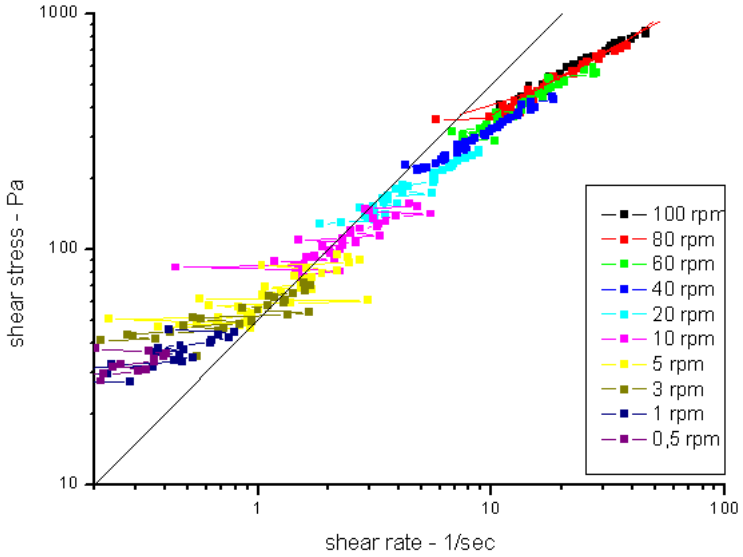

Figure 4.30: Flow curve of a suspension of 47 vol.% Durcal 5 with the glucose-water mixture after 15 hours of idle time with shear stress on y-axis and shear rate on x-axis.

deviation is visible. This deviation could be caused by the exceeding of the Tylor-Number and the appearance of perturbations and turbulence in the sample caused by high centrifugal forces. At lower speed, a flattening of the curve can be observed. Due to the remaining problem concerning torque measurement, the other results of the fresh sample, the sample after 66 hours of rest and the sample with Glenium were excluded from the report.

4.8.1.7 Conclusion

The assumed linear flow profile at a standard rheometer measurement can be overcome which helps to study complex fluids. To improve the quality of measurement, a temperature controlling system should be developed for further measurements at suspensions with very high viscosity.

5 Conclusion

The analysis of the flocculation and its structure formation process in a dense opaque suspension is a very complex problem.

First of all, the repeatability of measurements must be guaranteed. Thus, it is vitally important to obtain compareable results by the elimination of systematical errors like change in viscosity of the glucose-water mixture, introduction of impurities (alkalies) concerning flocculation, change in temperature at measurement and also exposure of calcium carbonate to humidity.

Second, the direct observation of the flocculation process in a dense opaque suspension is difficult to achieve by optical devices due to the opacity of the suspension.

At **transmitted light microscopy**, only the surface of the suspension can be observed with a depth of some micrometer. This is not representative for the whole sample and doesn't give information about agglomeration and structure formation in the suspension. Dilution of the dense opaque suspension makes direct observation of flocs possible and enable monitoring of floc size and floc structure. However, the impact of the dilution on the floc structure is not known.

The **confocal microscope** is not capable to observe an evolution process of flocculation or already present floc structure in the model suspension without dilution. The confocal microscope could be a powerful device for the study of floc structure in a diluted suspension due to its higher resolution in the profundity of a sample and the possible creation of a 3D-model.

The **laser particle size analyser** is capable to measure a particle size distribution in a dense opaque suspension by diluting the dense suspension in the testing liquid. However, the impact on flocs caused by dilution/pumping of the liquid should be investigated as well as the impact of model-dependency. The impact of influencing factors could be estimated through the comparison of measurement data with the average particle size observed in the transmitted light microscope.

The **Turbiscan** device from Formulaction is a stability measurement device. It does measure the average particle size but can not observe an evolution process in the sample and doesn't consequently obtain useful data for numerical modelling. Moreover, the measurement is strongly model dependent.

The combination of **FBRM®** and **PVM®** is a fast in-situ measurement method for dense opaque suspensions which gives the information of particle size distribution. It was not possible to distinguish in the model suspension in between agglomerated particles on flocs and free particles or between flocs qualitatively. The problem was the low distance between particles and the shape of flocs. A dilution of the sample with water or glucose-water mixture can help, because bonded particles are agglomerated to flocs and can be identified and measured more easily by increasing distance between particles/flocs. The FBRM® and PVM® has the advantage of measuring the particle size distribution by the rotating laser beam of the FBRM® and analysing possible floc structure at the same time at the PVM® image. It has further a reduced mechanical impact compared to the impact by the pump of the laser particle size analyser. A problem is the low contrast between the white calcium carbonate particles and the glucose-water liquid in the PVM® image. A fluorescence agent could improve the contrast.

The resolution of the X-ray source used in the **X-ray microtomography** was not high enough to observe particles or flocs. It can easily penetrate the sample but has the disadvantage of 3 hours of measurement time, which makes it only usable at already completely stable suspensions. The X-ray microtomography in the laboratory can help to study final flocculated structure in the suspension. A **Synchrotron X-ray** beam reduces testing time down to one second, which can help to study floc and structure formation at very small time steps. A possible disadvantage could be a problem to distinguish in dense suspensions in between flocs, structure and free particles, due to the low distance in between. The X-ray microtomography can possibly obtain very interesting information about flocculation by the use of a new X-ray source at Laboratory Navier with a resolution down to 0.25 μm.

The **Bruker Minispec** can measure an evolution process from a more homogenous to a heterogenous state. It can give information about the timescale of flocculation and local change in concentration. With a further improvement of the measurement, mathematical analysis and the use of the field gradient, it could possibly give some further information about floc structure.

The **rheometer** is a very exact measurement divice to follow an evolution process in a suspension. The temperature can be controlled precisely and the evolution of yield stress, loss and storage modulus can be measured. This helps to connect the influence of flocculation directly with the change of rheological properties with time.

The **Bruker Magnetic resonance imaging coupled with a rheometer** is a very powerful and unique measurement technique which is capable to measure the flow profile of a liquid rotated by a couette in a rheomter.

The MRI connected with the rheometer makes it possible to calculate a flow profile with the dependence of shear stress on shear rate. This helps to draw a conclusion concerning stability of flocs and gives very important information for the subsequent numerical modelling. A remaining problem is the installation of a temperature controlling system to avoid an increase of temperature during testing. Furthermore the torque measurement with the laboratory rheometer and the testing schedule have to be improved.

Figure 5.1 gives an overview of the tested devices with including their capability to describe a flocculating process

All devices show advantages and disadvantages. The data necessary for further numerical modelling will be gained by the evaluation and combination of results from different measurement devices. To study floc size and floc structure, the transmitted light microscope and confocal microscope will be used to observe a diluted suspension. The laser particle size analyser will be used to study floc size evolution. The X-ray microtomography could help to characterize final flocculated structure in the suspension and to follow flocculation probably directly at a Synchrotron radiation source. The rheometer and magnetic resonance imaging coupled with a rheometer will measure rheological properties of the suspension.

Device	performed at:	Durcal 5 content	idle time after preparation	diluted for observation		Glenium		what is measured:	suitable for flocculation	
		[vol. %]	[h]	yes	no	yes [%]	no		why	why not
Transmitted light microscopy	Ecole des Ponts ParisTech	47	0	x			x	floc size and structur	size and structure can be observed	
		47	24		x		x	floc size and structur		only surface observation
		47	24	x			x	floc size and structur	size and structure can be observed	
		47	24	x		1,80		floc size and structur	dispersed state can be observed	
		47	168	x			x	floc size and structur	size and structure can be observed	
Confocal microscopy	Agro ParisTech	42	24		x		x	floc size and structur		only surface observation
		47	24		x		x	floc size and structur		only surface observation
		47	24		x	1,80		floc size and structur		only surface observation
Turbiscan	Formulaction	40	120		x		x	average particle size		doesn't show sample evolution
		40	0		x		x	average particle size		doesn't show sample evolution
Laser particle size analyser	Ecole des Ponts ParisTech	42	24	x			x	floc size distribution		vol. fraction too low
		45	24	x			x	floc size distribution	does measure evolution in floc size	
		45	24	x		1,80		floc size distribution	does measure original particle size	
		47	24	x			x	floc size distribution	does measure evolution in floc size	
FBRM®	Mettler and Toledo - ENPC	42	72		x		x	floc size distribution		too dense suspension, not diluted
		47	0		x		x	floc size distribution		too dense suspension, not diluted
		47	72		x		x	floc size distribution		too dense suspension, not diluted
		47	72		x	1,80		floc size distribution		too dense suspension, not diluted
PVM®	Mettler and Toledo - ENPC	42	72		x		x	floc structure		no contrast
		47	0		x		x	floc structure		no contrast
		47	72		x		x	floc structure		no contrast
		47	72		x	1,80		floc structure		no contrast
X-ray Microtomography	Ecole des Ponts ParisTech	47	72		x		x	structure		resolution not high enough
Rheometry	Ecole des Ponts ParisTech	43	various		x	both		yield stress, G', G''	does measure yieldstress, G', G'' evolution	
		47	various		x	both		yield stress, G', G''	does measure yieldstress, G', G'' evolution	
Minispec	Ecole des Ponts ParisTech	30	0		x		x	concentration change	does measure local concentration change with time	
		40	0		x		x	concentration change	does measure local concentration change with time	
		47	0		x		x	concentration change	does measure local concentration change with time	
		47	0		x	1,80		concentration change	does measure local concentration change with time	
MRI coupled with Rheometer	Ecole des Ponts ParisTech	47	15		x		x	concentration and velocity profile	concentration profile -> no sedimentation, velocity profile: flow curve calculation	

Figure 5.1: Conclusion concerning flocculation measurement for the different tested devices.

Bibliography

1 A.J. Allen and J.J. Thomas. Analysis of c–s–h gel and cement paste by small-angle neutron scattering. *Cement and concrete research*, 37(3):319–324, 2007. 2.2.11

2 H.A. Barnes. Thixotropy–a review. *Journal of Non-Newtonian Fluid Mechanics*, 70(1-2):1–33, 1997. 2.1, 2.1, 4.7.2, 4.7.3

3 BASF. Glenium® 7700. Technical report, BASF. 3.1.5

4 A. Blanco, E. Fuente, C. Negro, and J. Tijero. Flocculation monitoring: focused beam reflectance measurement as a measurement tool. *The Canadian Journal of Chemical Engineering*, 80(4):1–7, 2002. 2.2.8

5 EHC Bromley and I. Hopkinson. Confocal microscopy of a dense particle system. *Journal of colloid and interface science*, 245(1):75–80, 2002. 2.2.5

6 Torsten Hofmann Dr. Dieter Jehnichen. X-ray lab. Technical report, Leibnitz - Institut fuer Polymerforschung Dresden, 2012. 2.8

7 L. Ferrari, J. Kaufmann, F. Winnefeld, and J. Plank. Interaction of cement model systems with superplasticizers investigated by atomic force microscopy, zeta potential, and adsorption measurements. *Journal of Colloid and Interface Science*, 347(1):15–24, 2010. 2.4, 2.2.6

8 Formulaction. Turbiscan - the reference for stability analysis. Technical report, Formulaction - Smart scientific analysis. 2.2.10, 2.7, 4.3

9 Hamid Hafid. *Influence des paramètres morphologiques des granulats sur le comportement rhéologique des bétons frais : étude sur systèmes modéles*. PhD thesis, Université Paris-Est, Ecole Doctorale des Sciences, Ingénierie et Environnement, 2012. 2.12, 4.8.1

10 Ian Haley. Brief introduction to mettler-toledo fbrm® and pvm®. Technical report, Mettler-Toledo, 2012. 2.5, 2.6, 4.8

11 Benoit Faure Ian Haley. Tracking flocculation behaviour using fbrm and pvm in-situ particle characterisation. Technical report, Mettler-Toledo, 2012. 4.5.2, 4.11, 4.12

12 S. Jeremy. Essential techniques: Confocal microscopy. Technical report, www.microscopist.co.uk. 2.3

13 MCG Juenger, VHR Lamour, PJM Monteiro, EM Gartner, and GP Denbeaux. Direct observation of cement hydration by soft x-ray transmission microscopy. *Journal of materials science letters*, 22(19):1335–1337, 2003. 2.2.3, 2.2.4, 2.2, 2.2.4

14 R.A. Ketcham and W.D. Carlson. Acquisition, optimization and interpretation of x-ray computed tomographic imagery: applications to the geosciences. *Computers & Geosciences*, 27(4):381–400, 2001. 2.2.12

15 C. Kunz and K. Codling. *Synchrotron radiation*. Springer, 1979. 2.2.4

16 E.N. Landis and D.T. Keane. X-ray microtomography. *Materials Characterization*, 61(12):1305–1316, 2010. 2.2.12

17 Nicolas Lenoir. Basics of x-ray computed tomography. Technical report, Laboratoire Navier, 2012. 2.2.12

18 Fabien Mahaut. *Comportement rhéologique de suspension de partcules non colloïdales plongées dans des fluides à seuil*. PhD thesis, Docteur de L'Universite Paris-Est, 2009. 4.8.1

19 Malvern. *Laser Diffraction - Particle size distributions from nanometers to millimeters*. Malvern Instruments Ltd, Enigma Business Park Grovewood Road Malvern Worcestershire WR14 1XZ United Kingdom. 2.2.7

20 Julie Goyon Xavier Chateau Olivier Pitois Guillaume Ovarlez Michael Kogan, Lucie Ducloue. Mixtures of foam and paste: suspensions of bubbles in yield stress fluids. 4.7.3

21 G. Ovarlez, F. Bertrand, and S. Rodts. Local determination of the constitutive law of a dense suspension of non-colloidal particles through mri. *arXiv preprint cond-mat/0509336*, 2005. 4.8.1.3, 4.8.1.5

22 F. Pignon, A. Magnin, J.M. Piau, B. Cabane, P. Lindner, and O. Diat. Yield stress thixotropic clay suspension: Investigations of structure by light, neutron, and x-ray scattering. *Physical Review E*, 56(3):3281, 1997. 4.7.3

23 Stéphane RODTS. Irm tour dhorizon. Technical report, Navier, CNRS, Paris Tech, 2009. 2.9, 2.10

24 D. Rugar and P. Hansma. Atomic force microscopy. *Phys. Today*, 43(10):23–30, 1990. 2.2.6

25 Alex Grishaev Xiaobing Zuo. The first nih workshop on small angle x-ray scattering and application in biomolecular studies. 2009. 2.8